Structure theory of parabolic nodal and singular sets

Robert Koirala (UCSD)
(Joint work with Max Hallgren and Zilu Ma)

Geometry and volume of $Z(u)$ and $S(u)$: polynomial case

For a nonzero function $u : \mathbb{R}^n \times \mathbb{R} \to \mathbb{R}$, define

$$Z(u) := \{u = 0\}, \qquad S(u) := \{u = 0,\ |\nabla u| = 0\}.$$

$u = x^2 + 2t$

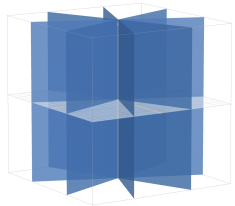

$u = x^4 - 6x^2y^2 + y^4$

- For polynomial u, $Z(u) \setminus S(u)$ **is a real analytic hypersurface**; $\operatorname{codim}(Z(u)) \geq 1$, $\operatorname{codim}(S(u)) \geq 2$.
- Wongkew ('93): $\operatorname{Vol}\big(P_r(Z(u) \cap P_1)\big) \lesssim_d r$, $\operatorname{Vol}\big(P_r(S(u) \cap P_1)\big) \lesssim_d r^2$, d is degree of u

Which geometric and measure-theoretic features persist beyond the polynomial setting?

Geometry and volume of $Z(u)$ and $S(u)$: polynomial case

For a nonzero function $u : \mathbb{R}^n \times \mathbb{R} \to \mathbb{R}$, define

$$Z(u) := \{u = 0\}, \qquad S(u) := \{u = 0,\ |\nabla u| = 0\}.$$

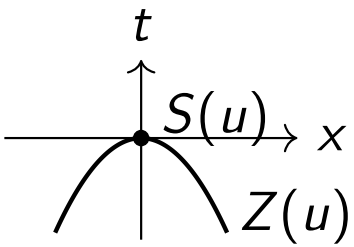

$u = x^2 + 2t$

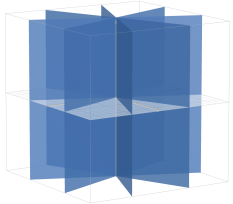

$u = x^4 - 6x^2y^2 + y^4$

- For polynomial u, $Z(u) \setminus S(u)$ **is a real analytic hypersurface**; $\operatorname{codim}(Z(u)) \geq 1$, $\operatorname{codim}(S(u)) \geq 2$.
- Wongkew ('93): $\operatorname{Vol}\big(P_r(Z(u) \cap P_1)\big) \lesssim_d r$, $\operatorname{Vol}\big(P_r(S(u) \cap P_1)\big) \lesssim_d r^2$, d is degree of u

Which geometric and measure-theoretic features persist beyond the polynomial setting?

Geometry and volume of $Z(u)$ and $S(u)$: polynomial case

For a nonzero function $u : \mathbb{R}^n \times \mathbb{R} \to \mathbb{R}$, define

$$Z(u) := \{u = 0\}, \qquad S(u) := \{u = 0,\ |\nabla u| = 0\}.$$

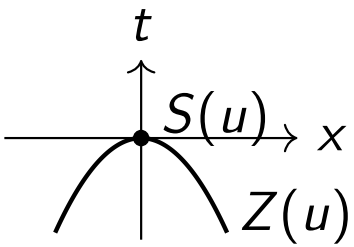

$u = x^2 + 2t$

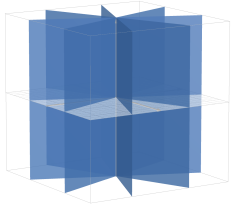

$u = x^4 - 6x^2y^2 + y^4$

- For polynomial u, $Z(u) \setminus S(u)$ **is a real analytic hypersurface**; $\operatorname{codim}(Z(u)) \geq 1$, $\operatorname{codim}(S(u)) \geq 2$.
- Wongkew ('93): $\operatorname{Vol}\big(P_r(Z(u) \cap P_1)\big) \lesssim_d r$, $\operatorname{Vol}\big(P_r(S(u) \cap P_1)\big) \lesssim_d r^2$, d is degree of u

Which geometric and measure-theoretic features persist beyond the polynomial setting?

Geometry and volume of $Z(u)$ and $S(u)$: polynomial case

For a nonzero function $u : \mathbb{R}^n \times \mathbb{R} \to \mathbb{R}$, define

$$Z(u) := \{u = 0\}, \qquad S(u) := \{u = 0,\ |\nabla u| = 0\}.$$

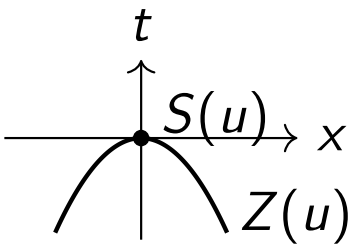

$u = x^2 + 2t$

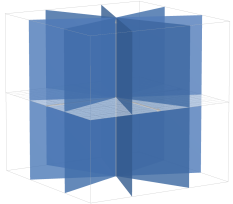

$u = x^4 - 6x^2y^2 + y^4$

- For polynomial u, $Z(u) \setminus S(u)$ **is a real analytic hypersurface**; $\operatorname{codim}(Z(u)) \geq 1$, $\operatorname{codim}(S(u)) \geq 2$.
- Wongkew ('93): $\operatorname{Vol}\big(P_r(Z(u) \cap P_1)\big) \lesssim_d r$, $\operatorname{Vol}\big(P_r(S(u) \cap P_1)\big) \lesssim_d r^2$, d is degree of u

Which geometric and measure-theoretic features persist beyond the polynomial setting?

Geometry and volume of $Z(u)$ and $S(u)$: polynomial case

For a nonzero function $u : \mathbb{R}^n \times \mathbb{R} \to \mathbb{R}$, define

$$Z(u) := \{u = 0\}, \qquad S(u) := \{u = 0,\ |\nabla u| = 0\}.$$

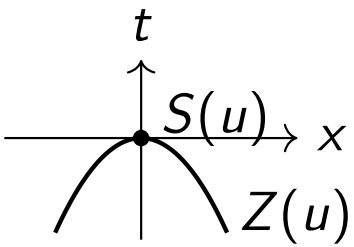

$u = x^2 + 2t$

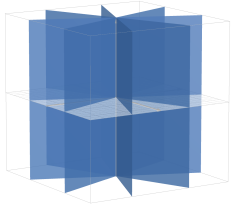

$u = x^4 - 6x^2y^2 + y^4$

- For polynomial u, $Z(u) \setminus S(u)$ **is a real analytic hypersurface**; $\operatorname{codim}(Z(u)) \geq 1$, $\operatorname{codim}(S(u)) \geq 2$.
- Wongkew ('93): $\operatorname{Vol}\big(P_r(Z(u) \cap P_1)\big) \lesssim_d r$, $\operatorname{Vol}\big(P_r(S(u) \cap P_1)\big) \lesssim_d r^2$, d is degree of u

Which geometric and measure-theoretic features persist beyond the polynomial setting?

Geometry and volume of $Z(u)$ and $S(u)$: polynomial case

For a nonzero function $u : \mathbb{R}^n \times \mathbb{R} \to \mathbb{R}$, define

$$Z(u) := \{u = 0\}, \qquad S(u) := \{u = 0,\ |\nabla u| = 0\}.$$

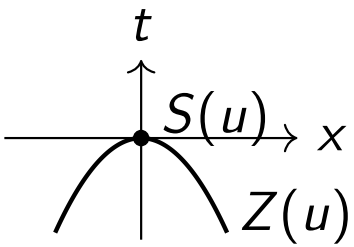

$u = x^2 + 2t$

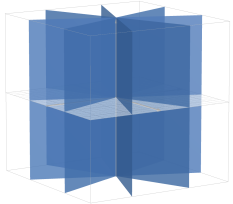

$u = x^4 - 6x^2y^2 + y^4$

- For polynomial u, $Z(u) \setminus S(u)$ **is a real analytic hypersurface**; $\operatorname{codim}(Z(u)) \geq 1$, $\operatorname{codim}(S(u)) \geq 2$.
- Wongkew ('93): $\operatorname{Vol}\big(P_r(Z(u) \cap P_1)\big) \lesssim_d r$, $\operatorname{Vol}\big(P_r(S(u) \cap P_1)\big) \lesssim_d r^2$, d is degree of u

Which geometric and measure-theoretic features persist beyond the polynomial setting?

Main results when u solves a parabolic inequality

Let u satisfy

$$|\partial_t u - \operatorname{div}(a(x,t)\nabla u)| \leq M\big(|u| + |\nabla u|\big) \tag{1}$$

on an open subset of $\mathbb{R}^n \times \mathbb{R}$, where $a = (a_{ij})$ is uniformly elliptic and

$$|a_{ij}(x,t) - a_{ij}(y,s)| \leq M \max\{|x-y|, \sqrt{|t-s|}\}.$$

Model case. When $M = 0$ and $a_{ij} = \delta_{ij}$, this is the heat equation $\partial_t u = \Delta u$, and u is **caloric**.

Main results (Hallgren–K.–Ma, 2025)

Main results when u solves a parabolic inequality

Let u satisfy

$$|\partial_t u - \operatorname{div}(a(x,t)\nabla u)| \le M\big(|u| + |\nabla u|\big) \tag{1}$$

on an open subset of $\mathbb{R}^n \times \mathbb{R}$, where $a = (a_{ij})$ is uniformly elliptic and

$$|a_{ij}(x,t) - a_{ij}(y,s)| \le M \max\{|x-y|, \sqrt{|t-s|}\}.$$

Model case. When $M = 0$ and $a_{ij} = \delta_{ij}$, this is the heat equation $\partial_t u = \Delta u$, and u is **caloric**.

Main results (Hallgren–K.–Ma, 2025)

Main results when u solves a parabolic inequality

Let u satisfy

$$|\partial_t u - \operatorname{div}(a(x,t)\nabla u)| \leq M\big(|u| + |\nabla u|\big) \tag{1}$$

on an open subset of $\mathbb{R}^n \times \mathbb{R}$, where $a = (a_{ij})$ is uniformly elliptic and

$$|a_{ij}(x,t) - a_{ij}(y,s)| \leq M \max\{|x-y|, \sqrt{|t-s|}\}.$$

Model case. When $M = 0$ and $a_{ij} = \delta_{ij}$, this is the heat equation $\partial_t u = \Delta u$, and u is **caloric**.

Main results (Hallgren–K.–Ma, 2025)

1. Up to negligible sets, $Z(u)$ and $S(u)$ are covered by a countable union of **regular parabolic Lipschitz graphs** of codimension 1 and 2, respectively.
2. **Space-time Minkowski estimates:**

$$\operatorname{Vol}\big(P_r(Z(u) \cap P(\mathbf{0},1))\big) \lesssim r, \qquad \operatorname{Vol}\big(P_r(S(u) \cap P(\mathbf{0},1))\big) \lesssim r^2,$$

with corresponding estimates for almost every time slice.

Main results when u solves a parabolic inequality

Let u satisfy

$$|\partial_t u - \operatorname{div}(a(x,t)\nabla u)| \leq M\big(|u| + |\nabla u|\big) \tag{1}$$

on an open subset of $\mathbb{R}^n \times \mathbb{R}$, where $a = (a_{ij})$ is uniformly elliptic and

$$|a_{ij}(x,t) - a_{ij}(y,s)| \leq M \max\{|x-y|, \sqrt{|t-s|}\}.$$

Model case. When $M = 0$ and $a_{ij} = \delta_{ij}$, this is the heat equation $\partial_t u = \Delta u$, and u is **caloric**.

Main results (Hallgren–K.–Ma, 2025)

1. Up to negligible sets, $Z(u)$ and $S(u)$ are covered by a countable union of **regular parabolic Lipschitz graphs** of codimension 1 and 2, respectively.
2. **Space-time Minkowski estimates:**

$$\operatorname{Vol}\big(P_r(Z(u) \cap P(\mathbf{0},1))\big) \lesssim r, \qquad \operatorname{Vol}\big(P_r(S(u) \cap P(\mathbf{0},1))\big) \lesssim r^2,$$

with corresponding estimates for almost every time slice.

Preview of the proof: zooming in and symmetry

- After **parabolic rescaling,** a solution u is well approximated at infinitesimal scales by a caloric polynomial.
- The **volume** of $Z(u)$ and $S(u)$ is a **dimensional** information, and dimension is reflected by the number of symmetries.

- If a nonzero caloric function is symmetric (invariant) in all space-time directions, then

$$\partial_t u = 0, \qquad |\nabla u| = 0,$$

so $u \equiv c \neq 0$ and hence $Z(u) = \emptyset$.

- If a caloric function is symmetric in all but one direction, then after rotation

$$\partial_t u = 0, \qquad \partial_i u = 0 \quad (1 \leq i \leq n-1).$$

Thus $u = u(x_n)$ and $\Delta u = 0$, so u is linear and therefore $S(u) = \emptyset$.

Maximal symmetry rules out nodal and singular sets.

Preview of the proof: zooming in and symmetry

- After **parabolic rescaling,** a solution u is well approximated at infinitesimal scales by a caloric polynomial.
- The **volume** of $Z(u)$ and $S(u)$ is a **dimensional** information, and dimension is reflected by the number of symmetries.

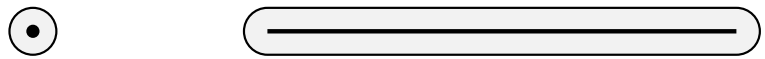

- If a nonzero caloric function is symmetric (invariant) in all space-time directions, then

$$\partial_t u = 0, \qquad |\nabla u| = 0,$$

so $u \equiv c \neq 0$ and hence $Z(u) = \emptyset$.

- If a caloric function is symmetric in all but one direction, then after rotation

$$\partial_t u = 0, \qquad \partial_i u = 0 \quad (1 \leq i \leq n-1).$$

Thus $u = u(x_n)$ and $\Delta u = 0$, so u is linear and therefore $S(u) = \emptyset$.

Maximal symmetry rules out nodal and singular sets.

Preview of the proof: zooming in and symmetry

- After **parabolic rescaling,** a solution u is well approximated at infinitesimal scales by a caloric polynomial.
- The **volume** of $Z(u)$ and $S(u)$ is a **dimensional** information, and dimension is reflected by the number of symmetries.

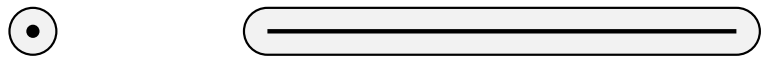

- If a nonzero caloric function is symmetric (invariant) in all space-time directions, then

$$\partial_t u = 0, \qquad |\nabla u| = 0,$$

so $u \equiv c \neq 0$ and hence $Z(u) = \emptyset$.

- If a caloric function is symmetric in all but one direction, then after rotation

$$\partial_t u = 0, \qquad \partial_i u = 0 \quad (1 \leq i \leq n-1).$$

Thus $u = u(x_n)$ and $\Delta u = 0$, so u is linear and therefore $S(u) = \emptyset$.

Maximal symmetry rules out nodal and singular sets.

Preview of the proof: zooming in and symmetry

- After **parabolic rescaling,** a solution u is well approximated at infinitesimal scales by a caloric polynomial.
- The **volume** of $Z(u)$ and $S(u)$ is a **dimensional** information, and dimension is reflected by the number of symmetries.

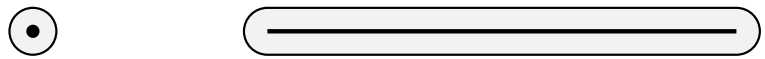

- If a nonzero caloric function is symmetric (invariant) in all space-time directions, then

$$\partial_t u = 0, \qquad |\nabla u| = 0,$$

so $u \equiv c \neq 0$ and hence $Z(u) = \emptyset$.

- If a caloric function is symmetric in all but one direction, then after rotation

$$\partial_t u = 0, \qquad \partial_i u = 0 \quad (1 \leq i \leq n-1).$$

Thus $u = u(x_n)$ and $\Delta u = 0$, so u is linear and therefore $S(u) = \emptyset$.

Maximal symmetry rules out nodal and singular sets.

Preview of the proof: zooming in and symmetry

- After **parabolic rescaling,** a solution u is well approximated at infinitesimal scales by a caloric polynomial.
- The **volume** of $Z(u)$ and $S(u)$ is a **dimensional** information, and dimension is reflected by the number of symmetries.

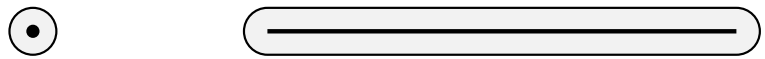

- If a nonzero caloric function is symmetric (invariant) in all space-time directions, then

$$\partial_t u = 0, \qquad |\nabla u| = 0,$$

  so $u \equiv c \neq 0$ and hence $Z(u) = \emptyset$.
- If a caloric function is symmetric in all but one direction, then after rotation

$$\partial_t u = 0, \qquad \partial_i u = 0 \quad (1 \leq i \leq n-1).$$

  Thus $u = u(x_n)$ and $\Delta u = 0$, so u is linear and therefore $S(u) = \emptyset$.

Maximal symmetry rules out nodal and singular sets.

Roadmap: detect polynomial behavior and symmetry

Parabolic analogue of the quantitative stratification of Cheeger, Jiang, Naber, and Valtorta.

1. Introduction: Structure of nodal and singular sets
2. History
3. Frequency detects polynomial behavior and symmetry
4. Quantitative strata and ε-regularity
5. Neck regions organize multiscale polynomial behavior and symmetry
6. General setting

Parabolic obstruction: Regularity in time is subtler. Controlling the half-time derivative $\partial_t^{1/2}$ is the main new difficulty. Also, errors must be summable across scales.

Roadmap: detect polynomial behavior and symmetry

Parabolic analogue of the quantitative stratification of Cheeger, Jiang, Naber, and Valtorta.

1. Introduction: Structure of nodal and singular sets
2. History
3. Frequency detects polynomial behavior and symmetry
4. Quantitative strata and ε-regularity
5. Neck regions organize multiscale polynomial behavior and symmetry
6. General setting

Parabolic obstruction: Regularity in time is subtler. Controlling the half-time derivative $\partial_t^{1/2}$ is the main new difficulty. Also, errors must be summable across scales.

Where does our work fit in the literature?

- In the 1990s, Han and Lin proved Euclidean Hausdorff estimates for $Z(u)$ and obtained non-optimal dimensional bounds for $S(u)$.
- There is an extensive work in both the elliptic and parabolic settings: Donnelly and Fefferman 90s, Logunov '18, Logunov and Malinnikova 20s, and many others.
- Cheeger, Naber, Valtorta (2015) proved optimal-dimensional Minkowski estimates and rectifiability for critical sets in the elliptic setting.
- Huang and Jiang (2024) proved sharp Hausdorff estimates for time-slices $Z(u) \cap \{t = \text{const}\}$ in the parabolic setting.
- Related ideas from **quantitative stratification** and **neck decomposition** have been used in parabolic problems such as mean curvature flow, harmonic map heat flow, and Ricci flow, as well as in elliptic problems such as harmonic maps, minimal surfaces, and spaces with lower Ricci curvature bounds.
- Optimal dimensional bounds for $S(u)$, parabolic Minkowski estimates for both sets, and time-slice estimates for $S(u)$ were missing until now.

Where does our work fit in the literature?

- In the 1990s, Han and Lin proved Euclidean Hausdorff estimates for $Z(u)$ and obtained non-optimal dimensional bounds for $S(u)$.
- There is an extensive work in both the elliptic and parabolic settings: Donnelly and Fefferman 90s, Logunov '18, Logunov and Malinnikova 20s, and many others.
- Cheeger, Naber, Valtorta (2015) proved optimal-dimensional Minkowski estimates and rectifiability for critical sets in the elliptic setting.
- Huang and Jiang (2024) proved sharp Hausdorff estimates for time-slices $Z(u) \cap \{t = \text{const}\}$ in the parabolic setting.
- Related ideas from **quantitative stratification** and **neck decomposition** have been used in parabolic problems such as mean curvature flow, harmonic map heat flow, and Ricci flow, as well as in elliptic problems such as harmonic maps, minimal surfaces, and spaces with lower Ricci curvature bounds.
- Optimal dimensional bounds for $S(u)$, parabolic Minkowski estimates for both sets, and time-slice estimates for $S(u)$ were missing until now.

Where does our work fit in the literature?

- In the 1990s, Han and Lin proved Euclidean Hausdorff estimates for $Z(u)$ and obtained non-optimal dimensional bounds for $S(u)$.
- There is an extensive work in both the elliptic and parabolic settings: Donnelly and Fefferman 90s, Logunov '18, Logunov and Malinnikova 20s, and many others.
- Cheeger, Naber, Valtorta (2015) proved optimal-dimensional Minkowski estimates and rectifiability for critical sets in the elliptic setting.
- Huang and Jiang (2024) proved sharp Hausdorff estimates for time-slices $Z(u) \cap \{t = \text{const}\}$ in the parabolic setting.
- Related ideas from **quantitative stratification** and **neck decomposition** have been used in parabolic problems such as mean curvature flow, harmonic map heat flow, and Ricci flow, as well as in elliptic problems such as harmonic maps, minimal surfaces, and spaces with lower Ricci curvature bounds.
- Optimal dimensional bounds for $S(u)$, parabolic Minkowski estimates for both sets, and time-slice estimates for $S(u)$ were missing until now.

Where does our work fit in the literature?

- In the 1990s, Han and Lin proved Euclidean Hausdorff estimates for $Z(u)$ and obtained non-optimal dimensional bounds for $S(u)$.
- There is an extensive work in both the elliptic and parabolic settings: Donnelly and Fefferman 90s, Logunov '18, Logunov and Malinnikova 20s, and many others.
- Cheeger, Naber, Valtorta (2015) proved optimal-dimensional Minkowski estimates and rectifiability for critical sets in the elliptic setting.
- Huang and Jiang (2024) proved sharp Hausdorff estimates for time-slices $Z(u) \cap \{t = \text{const}\}$ in the parabolic setting.
- Related ideas from **quantitative stratification** and **neck decomposition** have been used in parabolic problems such as mean curvature flow, harmonic map heat flow, and Ricci flow, as well as in elliptic problems such as harmonic maps, minimal surfaces, and spaces with lower Ricci curvature bounds.
- Optimal dimensional bounds for $S(u)$, parabolic Minkowski estimates for both sets, and time-slice estimates for $S(u)$ were missing until now.

Where does our work fit in the literature?

- In the 1990s, Han and Lin proved Euclidean Hausdorff estimates for $Z(u)$ and obtained non-optimal dimensional bounds for $S(u)$.
- There is an extensive work in both the elliptic and parabolic settings: Donnelly and Fefferman 90s, Logunov '18, Logunov and Malinnikova 20s, and many others.
- Cheeger, Naber, Valtorta (2015) proved optimal-dimensional Minkowski estimates and rectifiability for critical sets in the elliptic setting.
- Huang and Jiang (2024) proved sharp Hausdorff estimates for time-slices $Z(u) \cap \{t = \text{const}\}$ in the parabolic setting.
- Related ideas from **quantitative stratification** and **neck decomposition** have been used in parabolic problems such as mean curvature flow, harmonic map heat flow, and Ricci flow, as well as in elliptic problems such as harmonic maps, minimal surfaces, and spaces with lower Ricci curvature bounds.
- Optimal dimensional bounds for $S(u)$, parabolic Minkowski estimates for both sets, and time-slice estimates for $S(u)$ were missing until now.

Where does our work fit in the literature?

- In the 1990s, Han and Lin proved Euclidean Hausdorff estimates for $Z(u)$ and obtained non-optimal dimensional bounds for $S(u)$.
- There is an extensive work in both the elliptic and parabolic settings: Donnelly and Fefferman 90s, Logunov '18, Logunov and Malinnikova 20s, and many others.
- Cheeger, Naber, Valtorta (2015) proved optimal-dimensional Minkowski estimates and rectifiability for critical sets in the elliptic setting.
- Huang and Jiang (2024) proved sharp Hausdorff estimates for time-slices $Z(u) \cap \{t = \text{const}\}$ in the parabolic setting.
- Related ideas from **quantitative stratification** and **neck decomposition** have been used in parabolic problems such as mean curvature flow, harmonic map heat flow, and Ricci flow, as well as in elliptic problems such as harmonic maps, minimal surfaces, and spaces with lower Ricci curvature bounds.
- Optimal dimensional bounds for $S(u)$, parabolic Minkowski estimates for both sets, and time-slice estimates for $S(u)$ were missing until now.

The parabolic setting is different due to anisotropy in time

Natural space-time geometry: The parabolic metric $|(x,t)|_{\mathcal{P}}^2 = \max\{|x|^2, |t|\}$ is adapted to the scaling $(x,t) \mapsto (\lambda x, \lambda^2 t)$. In this geometry, time counts like two spatial dimensions.

A new regularity issue. Parabolic Lipschitz regularity gives only 1/2-Hölder control in time. The stronger notion of a **regular parabolic Lipschitz graph** requires $\partial_t^{1/2} u \in \mathrm{BMO}$, which is the **natural class in parabolic boundary value theory.** *This stronger class has* **no elliptic analogue** *and does not appear in earlier parabolic treatments of nodal and singular sets that we are aware of.*

Why time slice estimates are subtle. Since $Z_t(u) = S_t(u)$ in some cases, sharp time-slice estimates for $S(u)$ is genuinely delicate.

The parabolic setting is different due to anisotropy in time

Natural space-time geometry: The parabolic metric $|(x,t)|_{\mathcal{P}}^2 = \max\{|x|^2, |t|\}$ is adapted to the scaling $(x,t) \mapsto (\lambda x, \lambda^2 t)$. In this geometry, time counts like two spatial dimensions.

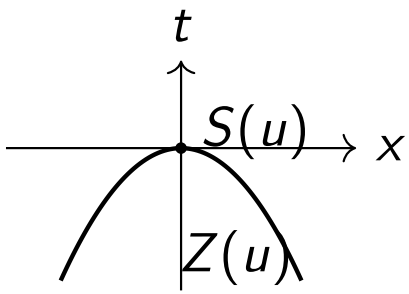

A new regularity issue. Parabolic Lipschitz regularity gives only 1/2-Hölder control in time. The stronger notion of a **regular parabolic Lipschitz graph** requires $\partial_t^{1/2} u \in \mathrm{BMO}$, which is the **natural class in parabolic boundary value theory.** *This stronger class has* **no elliptic analogue** *and does not appear in earlier parabolic treatments of nodal and singular sets that we are aware of.*

Why time slice estimates are subtle. Since $Z_t(u) = S_t(u)$ in some cases, sharp time-slice estimates for $S(u)$ is genuinely delicate.

The parabolic setting is different due to anisotropy in time

Natural space-time geometry: The parabolic metric $|(x,t)|_{\mathcal{P}}^2 = \max\{|x|^2, |t|\}$ is adapted to the scaling $(x,t) \mapsto (\lambda x, \lambda^2 t)$. In this geometry, time counts like two spatial dimensions.

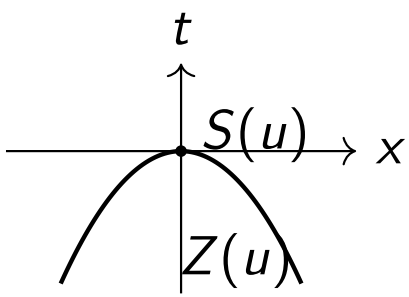

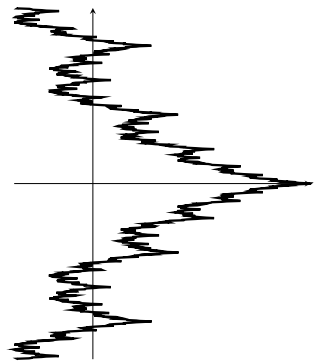

A new regularity issue. Parabolic Lipschitz regularity gives only 1/2-Hölder control in time. The stronger notion of a **regular parabolic Lipschitz graph** requires $\partial_t^{1/2} u \in \mathrm{BMO}$, which is the **natural class in parabolic boundary value theory.** *This stronger class has* **no elliptic analogue** *and does not appear in earlier parabolic treatments of nodal and singular sets that we are aware of.*

Why time slice estimates are subtle. Since $Z_t(u) = S_t(u)$ in some cases, sharp time-slice estimates for $S(u)$ is genuinely delicate.

The parabolic setting is different due to anisotropy in time

Natural space-time geometry: The parabolic metric $|(x,t)|_{\mathcal{P}}^2 = \max\{|x|^2, |t|\}$ is adapted to the scaling $(x,t) \mapsto (\lambda x, \lambda^2 t)$. In this geometry, time counts like two spatial dimensions.

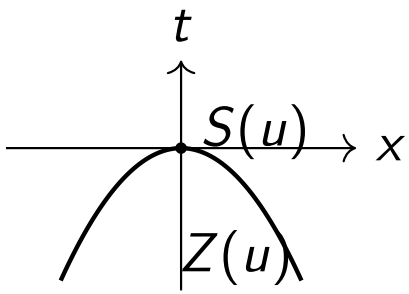

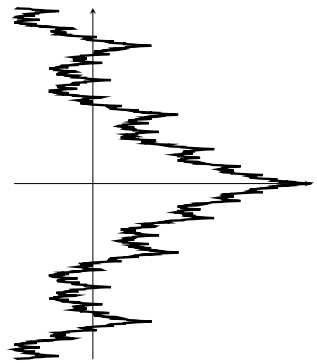

A new regularity issue. Parabolic Lipschitz regularity gives only 1/2-Hölder control in time. The stronger notion of a **regular parabolic Lipschitz graph** requires $\partial_t^{1/2} u \in \mathrm{BMO}$, which is the **natural class in parabolic boundary value theory.** *This stronger class has* **no elliptic analogue** *and does not appear in earlier parabolic treatments of nodal and singular sets that we are aware of.*

Why time slice estimates are subtle. Since $Z_t(u) = S_t(u)$ in some cases, sharp time-slice estimates for $S(u)$ is genuinely delicate.

The parabolic setting is different due to anisotropy in time

Natural space-time geometry: The parabolic metric $|(x,t)|_{\mathcal{P}}^2 = \max\{|x|^2, |t|\}$ is adapted to the scaling $(x,t) \mapsto (\lambda x, \lambda^2 t)$. In this geometry, time counts like two spatial dimensions.

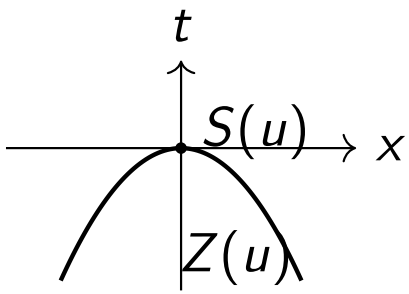

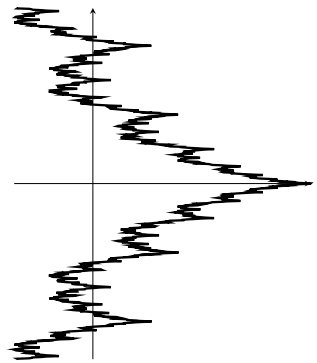

A new regularity issue. Parabolic Lipschitz regularity gives only 1/2-Hölder control in time. The stronger notion of a **regular parabolic Lipschitz graph** requires $\partial_t^{1/2} u \in \mathrm{BMO}$, which is the **natural class in parabolic boundary value theory.** *This stronger class has* **no elliptic analogue** *and does not appear in earlier parabolic treatments of nodal and singular sets that we are aware of.*

Why time slice estimates are subtle. Since $Z_t(u) = S_t(u)$ in some cases, sharp time-slice estimates for $S(u)$ is genuinely delicate.

The parabolic setting is different due to anisotropy in time

Natural space-time geometry: The parabolic metric $|(x,t)|_{\mathcal{P}}^2 = \max\{|x|^2, |t|\}$ is adapted to the scaling $(x,t) \mapsto (\lambda x, \lambda^2 t)$. In this geometry, time counts like two spatial dimensions.

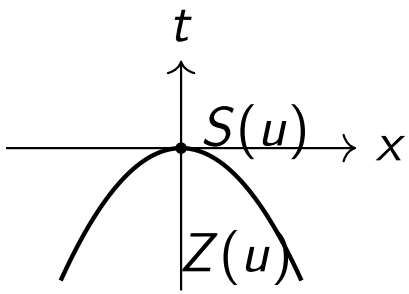

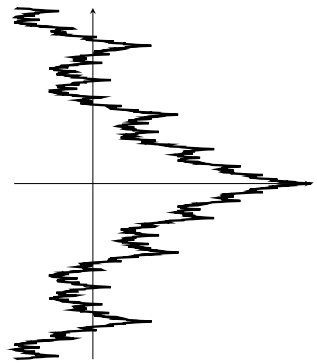

A new regularity issue. Parabolic Lipschitz regularity gives only 1/2-Hölder control in time. The stronger notion of a **regular parabolic Lipschitz graph** requires $\partial_t^{1/2} u \in \mathrm{BMO}$, which is the **natural class in parabolic boundary value theory.** *This stronger class has* **no elliptic analogue** *and does not appear in earlier parabolic treatments of nodal and singular sets that we are aware of.*

Why time slice estimates are subtle. Since $Z_t(u) = S_t(u)$ in some cases, sharp time-slice estimates for $S(u)$ is genuinely delicate.

Frequency, a parabolic analog of degree, is monotone

Fix $\mathbf{x}_0 := (x_0, t_0)$ and write $\tau = t_0 - t > 0$. Define

$$d\nu_{\mathbf{x}_0;t}(x) = \frac{1}{(4\pi\tau)^{n/2}} e^{-f_{\mathbf{x}_0}}\, dx, \qquad f_{\mathbf{x}_0}(x,t) := \frac{|x - x_0|^2}{4\tau}.$$

Poon's **frequency** is

$$N_{\mathbf{x}_0}(\tau) = \frac{2\tau \int_{\mathbb{R}^n} |\nabla u|^2 \, d\nu_{\mathbf{x}_0;t}}{\int_{\mathbb{R}^n} u^2 \, d\nu_{\mathbf{x}_0;t}} =: \frac{E_{\mathbf{x}_0}(\tau)}{H_{\mathbf{x}_0}(\tau)}.$$

Its derivative satisfies

$$N'_{\mathbf{x}_0}(\tau) = \frac{4\tau}{H_{\mathbf{x}_0}(\tau)} \int_{\mathbb{R}^n} \left(\left(\Delta_{f_{\mathbf{x}_0}} u + \frac{N_{\mathbf{x}_0}(\tau)}{2\tau} u \right)^2 + \left(\Delta_{f_{\mathbf{x}_0}} u + \frac{N_{\mathbf{x}_0}(\tau)}{2\tau} u \right) \Box u \right) d\nu_{\mathbf{x}_0;t},$$

where $\Delta_\phi := \Delta - \nabla\phi \cdot \nabla$ and $\Box u := \partial_t u - \Delta u$.

In the caloric case, $\Box u = 0$, so $N_{\mathbf{x}_0}(\tau)$ is monotone.

Frequency detects relative scale.

For the rest of the talk, we zoom in on the caloric setting.

Frequency, a parabolic analog of degree, is monotone

Fix $\mathbf{x}_0 := (x_0, t_0)$ and write $\tau = t_0 - t > 0$. Define

$$d\nu_{\mathbf{x}_0;t}(x) = \frac{1}{(4\pi\tau)^{n/2}} e^{-f_{\mathbf{x}_0}}\, dx, \qquad f_{\mathbf{x}_0}(x,t) := \frac{|x - x_0|^2}{4\tau}.$$

Poon's **frequency** is

$$N_{\mathbf{x}_0}(\tau) = \frac{2\tau \int_{\mathbb{R}^n} |\nabla u|^2 \, d\nu_{\mathbf{x}_0;t}}{\int_{\mathbb{R}^n} u^2 \, d\nu_{\mathbf{x}_0;t}} =: \frac{E_{\mathbf{x}_0}(\tau)}{H_{\mathbf{x}_0}(\tau)}.$$

Its derivative satisfies

$$N'_{\mathbf{x}_0}(\tau) = \frac{4\tau}{H_{\mathbf{x}_0}(\tau)} \int_{\mathbb{R}^n} \left(\left(\Delta_{f_{\mathbf{x}_0}} u + \frac{N_{\mathbf{x}_0}(\tau)}{2\tau} u \right)^2 + \left(\Delta_{f_{\mathbf{x}_0}} u + \frac{N_{\mathbf{x}_0}(\tau)}{2\tau} u \right) \Box u \right) d\nu_{\mathbf{x}_0;t},$$

where $\Delta_\phi := \Delta - \nabla\phi \cdot \nabla$ and $\Box u := \partial_t u - \Delta u$.

In the caloric case, $\Box u = 0$, so $N_{\mathbf{x}_0}(\tau)$ is monotone.

Frequency detects relative scale.

For the rest of the talk, we zoom in on the caloric setting.

Frequency, a parabolic analog of degree, is monotone

Fix $\mathbf{x}_0 := (x_0, t_0)$ and write $\tau = t_0 - t > 0$. Define

$$d\nu_{\mathbf{x}_0;t}(x) = \frac{1}{(4\pi\tau)^{n/2}} e^{-f_{\mathbf{x}_0}}\, dx, \qquad f_{\mathbf{x}_0}(x,t) := \frac{|x - x_0|^2}{4\tau}.$$

Poon's **frequency** is

$$N_{\mathbf{x}_0}(\tau) = \frac{2\tau \int_{\mathbb{R}^n} |\nabla u|^2 \, d\nu_{\mathbf{x}_0;t}}{\int_{\mathbb{R}^n} u^2 \, d\nu_{\mathbf{x}_0;t}} =: \frac{E_{\mathbf{x}_0}(\tau)}{H_{\mathbf{x}_0}(\tau)}.$$

Its derivative satisfies

$$N'_{\mathbf{x}_0}(\tau) = \frac{4\tau}{H_{\mathbf{x}_0}(\tau)} \int_{\mathbb{R}^n} \left(\left(\Delta_{f_{\mathbf{x}_0}} u + \frac{N_{\mathbf{x}_0}(\tau)}{2\tau} u \right)^2 + \left(\Delta_{f_{\mathbf{x}_0}} u + \frac{N_{\mathbf{x}_0}(\tau)}{2\tau} u \right) \Box u \right) d\nu_{\mathbf{x}_0;t},$$

where $\Delta_\phi := \Delta - \nabla\phi \cdot \nabla$ and $\Box u := \partial_t u - \Delta u$.

In the caloric case, $\Box u = 0$, so $N_{\mathbf{x}_0}(\tau)$ is monotone.

Frequency detects relative scale.

For the rest of the talk, we zoom in on the caloric setting.

Frequency, a parabolic analog of degree, is monotone

Fix $\mathbf{x}_0 := (x_0, t_0)$ and write $\tau = t_0 - t > 0$. Define

$$d\nu_{\mathbf{x}_0;t}(x) = \frac{1}{(4\pi\tau)^{n/2}} e^{-f_{\mathbf{x}_0}}\, dx, \qquad f_{\mathbf{x}_0}(x,t) := \frac{|x - x_0|^2}{4\tau}.$$

Poon's **frequency** is

$$N_{\mathbf{x}_0}(\tau) = \frac{2\tau \int_{\mathbb{R}^n} |\nabla u|^2 \, d\nu_{\mathbf{x}_0;t}}{\int_{\mathbb{R}^n} u^2 \, d\nu_{\mathbf{x}_0;t}} =: \frac{E_{\mathbf{x}_0}(\tau)}{H_{\mathbf{x}_0}(\tau)}.$$

Its derivative satisfies

$$N'_{\mathbf{x}_0}(\tau) = \frac{4\tau}{H_{\mathbf{x}_0}(\tau)} \int_{\mathbb{R}^n} \left(\left(\Delta_{f_{\mathbf{x}_0}} u + \frac{N_{\mathbf{x}_0}(\tau)}{2\tau} u \right)^2 + \left(\Delta_{f_{\mathbf{x}_0}} u + \frac{N_{\mathbf{x}_0}(\tau)}{2\tau} u \right) \Box u \right) d\nu_{\mathbf{x}_0;t},$$

where $\Delta_\phi := \Delta - \nabla\phi \cdot \nabla$ and $\Box u := \partial_t u - \Delta u$.

In the caloric case, $\Box u = 0$, so $N_{\mathbf{x}_0}(\tau)$ is monotone.

Frequency detects relative scale.

For the rest of the talk, we zoom in on the caloric setting.

Almost constant N implies almost homogeneity

$N_{\mathbf{x}_0}$ **is constant** if and only if $2\tau\Delta_{f_{\mathbf{x}_0}} u + N_{\mathbf{x}_0}(\tau)u = 0$, which forces u to be an m-**homogeneous caloric polynomial** p with $N_{\mathbf{x}_0}(\tau) \equiv m \in \mathbb{Z}_{\geq 0}$, i.e.,

$$\frac{p(x_0+\lambda(x-x_0),t_0+\lambda^2(t-t_0))}{\lambda^m} = p(x,t)$$

Theorem (Quantitative uniqueness of tangent flow in the caloric setting)

For any $0 < \tau < \tau_1/2 < \tau_2/4$, if $N_{\mathbf{x}_0}(\tau_2) - N_{\mathbf{x}_0}(\tau_1) < 1/10$, then there is $m \in \mathbb{Z}_{\geq 0}$ such that

$$\tau^{2l+j} \int_{\mathbb{R}^n} |\partial_t^l \nabla^j (u - p_m)|^2 \, d\nu_{\mathbf{x}_0;t} \leq C_{j,l}(N_{\mathbf{x}_0}(\tau_2) - N_{\mathbf{x}_0}(\tau_1))H_{\mathbf{x}_0}(\tau_2),$$

where p_m is the projection of u onto the eigenspace of $2\tau\Delta_{\mathbf{x}_0}$ with eigenvalue m.

Almost constant frequency means u is close to a homogeneous caloric polynomial.

Almost constant N implies almost homogeneity

$N_{\mathbf{x}_0}$ **is constant** if and only if $2\tau\Delta_{f_{\mathbf{x}_0}} u + N_{\mathbf{x}_0}(\tau)u = 0$, which forces u to be an m-**homogeneous caloric polynomial** p with $N_{\mathbf{x}_0}(\tau) \equiv m \in \mathbb{Z}_{\geq 0}$, i.e.,

$$\frac{p(x_0+\lambda(x-x_0),t_0+\lambda^2(t-t_0))}{\lambda^m} = p(x,t)$$

Theorem (Quantitative uniqueness of tangent flow in the caloric setting)

For any $0 < \tau < \tau_1/2 < \tau_2/4$, if $N_{\mathbf{x}_0}(\tau_2) - N_{\mathbf{x}_0}(\tau_1) < 1/10$, then there is $m \in \mathbb{Z}_{\geq 0}$ such that

$$\tau^{2l+j} \int_{\mathbb{R}^n} |\partial_t^l \nabla^j (u - p_m)|^2 \, d\nu_{\mathbf{x}_0;t} \leq C_{j,l}(N_{\mathbf{x}_0}(\tau_2) - N_{\mathbf{x}_0}(\tau_1))H_{\mathbf{x}_0}(\tau_2),$$

where p_m is the projection of u onto the eigenspace of $2\tau\Delta_{\mathbf{x}_0}$ with eigenvalue m.

Almost constant frequency means u is close to a homogeneous caloric polynomial.

Almost constant N implies almost homogeneity

$N_{\mathbf{x}_0}$ **is constant** if and only if $2\tau\Delta_{f_{\mathbf{x}_0}} u + N_{\mathbf{x}_0}(\tau)u = 0$, which forces u to be an m-**homogeneous caloric polynomial** p with $N_{\mathbf{x}_0}(\tau) \equiv m \in \mathbb{Z}_{\geq 0}$, i.e.,

$$\frac{p(x_0+\lambda(x-x_0),t_0+\lambda^2(t-t_0))}{\lambda^m} = p(x,t)$$

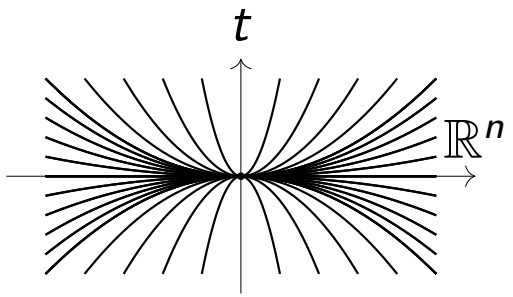

Theorem (Quantitative uniqueness of tangent flow in the caloric setting)

For any $0 < \tau < \tau_1/2 < \tau_2/4$, if $N_{\mathbf{x}_0}(\tau_2) - N_{\mathbf{x}_0}(\tau_1) < 1/10$, then there is $m \in \mathbb{Z}_{\geq 0}$ such that

$$\tau^{2l+j} \int_{\mathbb{R}^n} |\partial_t^l \nabla^j (u - p_m)|^2 \, d\nu_{\mathbf{x}_0;t} \leq C_{j,l}(N_{\mathbf{x}_0}(\tau_2) - N_{\mathbf{x}_0}(\tau_1))H_{\mathbf{x}_0}(\tau_2),$$

where p_m is the projection of u onto the eigenspace of $2\tau\Delta_{\mathbf{x}_0}$ with eigenvalue m.

Almost constant frequency means u is close to a homogeneous caloric polynomial.

Almost constant N implies almost homogeneity

$N_{\mathbf{x}_0}$ **is constant** if and only if $2\tau\Delta_{f_{\mathbf{x}_0}} u + N_{\mathbf{x}_0}(\tau)u = 0$, which forces u to be an m-**homogeneous caloric polynomial** p with $N_{\mathbf{x}_0}(\tau) \equiv m \in \mathbb{Z}_{\geq 0}$, i.e.,

$$\frac{p(x_0+\lambda(x-x_0),t_0+\lambda^2(t-t_0))}{\lambda^m} = p(x,t)$$

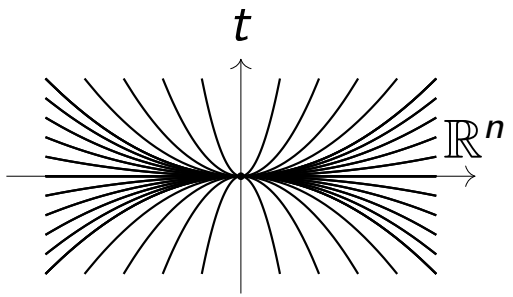

Theorem (Quantitative uniqueness of tangent flow in the caloric setting)

For any $0 < \tau < \tau_1/2 < \tau_2/4$, *if* $N_{\mathbf{x}_0}(\tau_2) - N_{\mathbf{x}_0}(\tau_1) < 1/10$, *then there is* $m \in \mathbb{Z}_{\geq 0}$ *such that*

$$\tau^{2l+j} \int_{\mathbb{R}^n} |\partial_t^l \nabla^j (u - p_m)|^2 \, d\nu_{\mathbf{x}_0;t} \leq C_{j,l}(N_{\mathbf{x}_0}(\tau_2) - N_{\mathbf{x}_0}(\tau_1))H_{\mathbf{x}_0}(\tau_2),$$

where p_m *is the projection of* u *onto the eigenspace of* $2\tau\Delta_{\mathbf{x}_0}$ *with eigenvalue* m.

Almost constant frequency means u is close to a homogeneous caloric polynomial.

Almost constant N implies almost homogeneity

$N_{\mathbf{x}_0}$ **is constant** if and only if $2\tau\Delta_{f_{\mathbf{x}_0}} u + N_{\mathbf{x}_0}(\tau)u = 0$, which forces u to be an m-**homogeneous caloric polynomial** p with $N_{\mathbf{x}_0}(\tau) \equiv m \in \mathbb{Z}_{\geq 0}$, i.e.,

$$\frac{p(x_0+\lambda(x-x_0),t_0+\lambda^2(t-t_0))}{\lambda^m} = p(x,t)$$

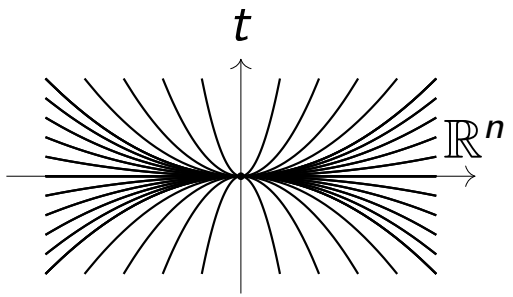

Theorem (Quantitative uniqueness of tangent flow in the caloric setting)

For any $0 < \tau < \tau_1/2 < \tau_2/4$, *if* $N_{\mathbf{x}_0}(\tau_2) - N_{\mathbf{x}_0}(\tau_1) < 1/10$, *then there is* $m \in \mathbb{Z}_{\geq 0}$ *such that*

$$\tau^{2l+j} \int_{\mathbb{R}^n} |\partial_t^l \nabla^j (u - p_m)|^2 \, d\nu_{\mathbf{x}_0;t} \leq C_{j,l}(N_{\mathbf{x}_0}(\tau_2) - N_{\mathbf{x}_0}(\tau_1))H_{\mathbf{x}_0}(\tau_2),$$

where p_m *is the projection of* u *onto the eigenspace of* $2\tau\Delta_{\mathbf{x}_0}$ *with eigenvalue* m.

Almost constant frequency means u is close to a homogeneous caloric polynomial.

Two homogeneities generate translation invariance

If N is constant at $\mathbf{x}_1 = (x_1, t_1)$ and $\mathbf{x}_2 = (x_2, t_2)$, then $2\tau_i \Delta_{f_i} u + mu = 0$ for $i \in \{1, 2\}$, for some $m \in \mathbb{Z}_{\geq 0}$, where $\tau_i = t_i - t$ and $f_i = f_{\mathbf{x}_i}$. We compute

$$\nabla u \cdot (x_2 - x_1) = 4\tau_2 \Delta_{f_2} u - 4\tau_1 \Delta_{f_1} u - [2\tau_1 \Delta_{f_1}, 2\tau_2 \Delta_{f_2}] u = 0,$$

$$2(t_2 - t_1)\partial_t u = [2\tau_1 \Delta_{f_1}, 2\tau_2 \Delta_{f_2}] u + 2\tau_1 \Delta_{f_1} u - 2\tau_2 \Delta_{f_2} u = 0.$$

Characteristic vector fields based at two points generate space–time directions.

Two homogeneities generate translation invariance

If N is constant at $\mathbf{x}_1 = (x_1, t_1)$ and $\mathbf{x}_2 = (x_2, t_2)$, then $2\tau_i \Delta_{f_i} u + mu = 0$ for $i \in \{1, 2\}$, for some $m \in \mathbb{Z}_{\geq 0}$, where $\tau_i = t_i - t$ and $f_i = f_{\mathbf{x}_i}$. We compute

$$\nabla u \cdot (x_2 - x_1) = 4\tau_2 \Delta_{f_2} u - 4\tau_1 \Delta_{f_1} u - [2\tau_1 \Delta_{f_1}, 2\tau_2 \Delta_{f_2}] u = 0,$$
$$2(t_2 - t_1)\partial_t u = [2\tau_1 \Delta_{f_1}, 2\tau_2 \Delta_{f_2}] u + 2\tau_1 \Delta_{f_1} u - 2\tau_2 \Delta_{f_2} u = 0.$$

Characteristic vector fields based at two points generate space–time directions.

Two homogeneities generate translation invariance

If N is constant at $\mathbf{x}_1 = (x_1, t_1)$ and $\mathbf{x}_2 = (x_2, t_2)$, then $2\tau_i \Delta_{f_i} u + mu = 0$ for $i \in \{1, 2\}$, for some $m \in \mathbb{Z}_{\geq 0}$, where $\tau_i = t_i - t$ and $f_i = f_{\mathbf{x}_i}$. We compute

$$\nabla u \cdot (x_2 - x_1) = 4\tau_2 \Delta_{f_2} u - 4\tau_1 \Delta_{f_1} u - [2\tau_1 \Delta_{f_1}, 2\tau_2 \Delta_{f_2}] u = 0,$$
$$2(t_2 - t_1)\partial_t u = [2\tau_1 \Delta_{f_1}, 2\tau_2 \Delta_{f_2}] u + 2\tau_1 \Delta_{f_1} u - 2\tau_2 \Delta_{f_2} u = 0.$$

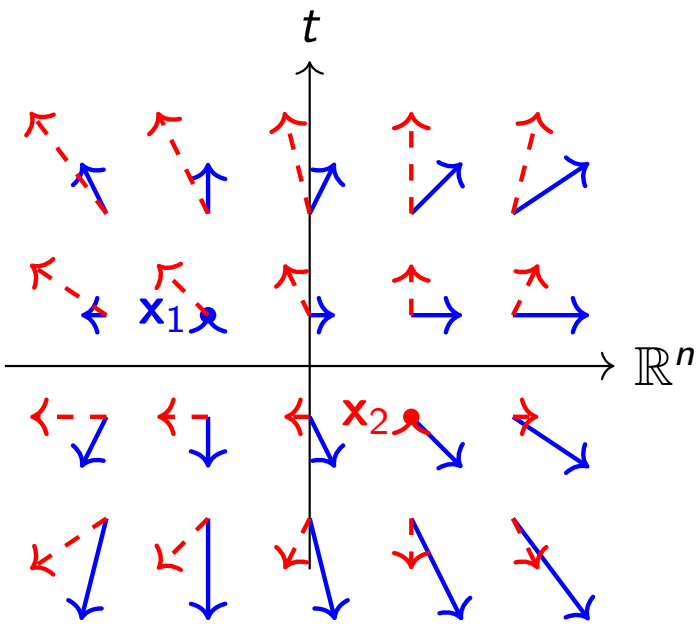

Characteristic vector fields based at two points generate space–time directions.

Two homogeneities generate translation invariance

If N is constant at $\mathbf{x}_1 = (x_1, t_1)$ and $\mathbf{x}_2 = (x_2, t_2)$, then $2\tau_i \Delta_{f_i} u + mu = 0$ for $i \in \{1, 2\}$, for some $m \in \mathbb{Z}_{\geq 0}$, where $\tau_i = t_i - t$ and $f_i = f_{\mathbf{x}_i}$. We compute

$$\nabla u \cdot (x_2 - x_1) = 4\tau_2 \Delta_{f_2} u - 4\tau_1 \Delta_{f_1} u - [2\tau_1 \Delta_{f_1}, 2\tau_2 \Delta_{f_2}] u = 0,$$
$$2(t_2 - t_1)\partial_t u = [2\tau_1 \Delta_{f_1}, 2\tau_2 \Delta_{f_2}] u + 2\tau_1 \Delta_{f_1} u - 2\tau_2 \Delta_{f_2} u = 0.$$

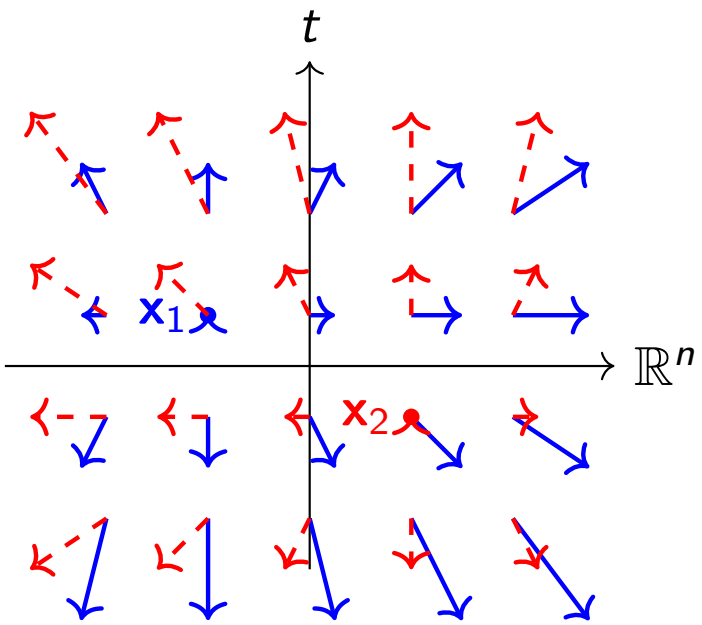

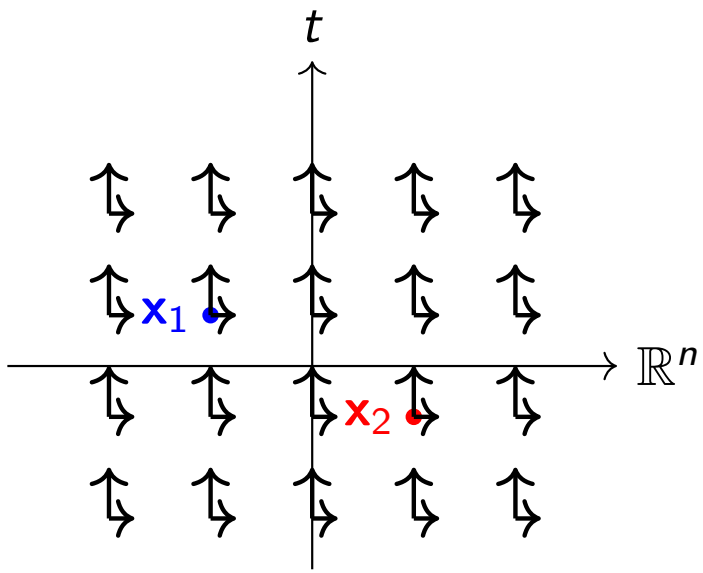

Characteristic vector fields based at two points generate space–time directions.

Two homogeneities generate translation invariance

If N is constant at $\mathbf{x}_1 = (x_1, t_1)$ and $\mathbf{x}_2 = (x_2, t_2)$, then $2\tau_i \Delta_{f_i} u + mu = 0$ for $i \in \{1, 2\}$, for some $m \in \mathbb{Z}_{\geq 0}$, where $\tau_i = t_i - t$ and $f_i = f_{\mathbf{x}_i}$. We compute

$$\nabla u \cdot (x_2 - x_1) = 4\tau_2 \Delta_{f_2} u - 4\tau_1 \Delta_{f_1} u - [2\tau_1 \Delta_{f_1}, 2\tau_2 \Delta_{f_2}] u = 0,$$
$$2(t_2 - t_1)\partial_t u = [2\tau_1 \Delta_{f_1}, 2\tau_2 \Delta_{f_2}] u + 2\tau_1 \Delta_{f_1} u - 2\tau_2 \Delta_{f_2} u = 0.$$

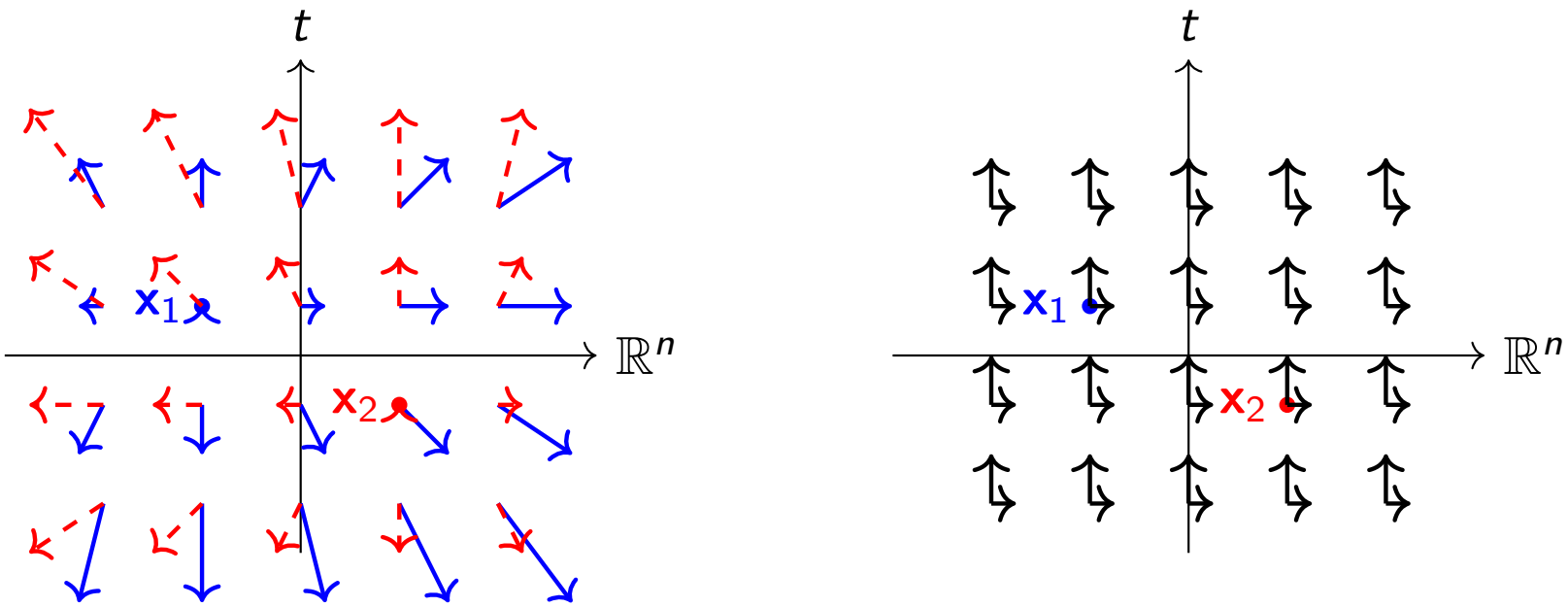

Characteristic vector fields based at two points generate space–time directions.

Homogeneity at many points forces space-time symmetry

An L^2 version of the previous argument yields the following.

Theorem (Cone splitting inequality)

Let u be a caloric function with $N_{\mathbf{x}_0}(10^5 r^2) \leq \Lambda$. If $\{\mathbf{x}_i\}_{i=0}^K \subset P(\mathbf{x}_0, \frac{1}{10}r)$ is $(k, \alpha r)$-independent and $K = k$, then

$$r^2 \int_{\mathbb{R}^n} |\pi_L \nabla u|^2 \, d\nu_{\mathbf{x}_0; t_0 - r^2} \leq C(\alpha, \Lambda) \max_i \left\{ N_{\mathbf{x}_i}(8r^2) - N_{\mathbf{x}_i}(r^2/8) \right\} \int_{\mathbb{R}^n} u^2 \, d\nu_{\mathbf{x}_0; t_0 - r^2},$$

where $L = \operatorname{Span}\{x_j - x_0\}_{j=0}^K$. If $\{\mathbf{x}_i\}_{i=0}^K$ is $(k, \alpha r)$-temporally independent and $K = k - 2$, we additionally have

$$r^4 \int_{\mathbb{R}^n} |\partial_t u|^2 \, d\nu_{\mathbf{x}_0; t_0 - r^2} \leq C(\alpha, \Lambda) \max_i \left\{ N_{\mathbf{x}_i}(8r^2) - N_{\mathbf{x}_i}(r^2/8) \right\} \int_{\mathbb{R}^n} u^2 \, d\nu_{\mathbf{x}_0; t_0 - r^2}.$$

Homogeneity at many well-separated points forces higher space-time symmetry.

Frequency detects both homogeneous polynomial behavior and space-time symmetry.

Homogeneity at many points forces space-time symmetry

An L^2 version of the previous argument yields the following.

Theorem (Cone splitting inequality)

Let u be a caloric function with $N_{\mathbf{x}_0}(10^5 r^2) \leq \Lambda$. If $\{\mathbf{x}_i\}_{i=0}^K \subset P(\mathbf{x}_0, \frac{1}{10}r)$ is $(k, \alpha r)$-independent and $K = k$, then

$$r^2 \int_{\mathbb{R}^n} |\pi_L \nabla u|^2 \, d\nu_{\mathbf{x}_0; t_0 - r^2} \leq C(\alpha, \Lambda) \max_i \left\{ N_{\mathbf{x}_i}(8r^2) - N_{\mathbf{x}_i}(r^2/8) \right\} \int_{\mathbb{R}^n} u^2 \, d\nu_{\mathbf{x}_0; t_0 - r^2},$$

where $L = \mathrm{Span}\{x_j - x_0\}_{j=0}^K$. If $\{\mathbf{x}_i\}_{i=0}^K$ is $(k, \alpha r)$-temporally independent and $K = k - 2$, we additionally have

$$r^4 \int_{\mathbb{R}^n} |\partial_t u|^2 \, d\nu_{\mathbf{x}_0; t_0 - r^2} \leq C(\alpha, \Lambda) \max_i \left\{ N_{\mathbf{x}_i}(8r^2) - N_{\mathbf{x}_i}(r^2/8) \right\} \int_{\mathbb{R}^n} u^2 \, d\nu_{\mathbf{x}_0; t_0 - r^2}.$$

Homogeneity at many well-separated points forces higher space-time symmetry.

Frequency detects both homogeneous polynomial behavior and space-time symmetry.

Homogeneity at many points forces space-time symmetry

An L^2 version of the previous argument yields the following.

Theorem (Cone splitting inequality)

Let u be a caloric function with $N_{\mathbf{x}_0}(10^5 r^2) \leq \Lambda$. If $\{\mathbf{x}_i\}_{i=0}^K \subset P(\mathbf{x}_0, \frac{1}{10}r)$ is $(k, \alpha r)$-independent and $K = k$, then

$$r^2 \int_{\mathbb{R}^n} |\pi_L \nabla u|^2 \, d\nu_{\mathbf{x}_0; t_0 - r^2} \leq C(\alpha, \Lambda) \max_i \left\{ N_{\mathbf{x}_i}(8r^2) - N_{\mathbf{x}_i}(r^2/8) \right\} \int_{\mathbb{R}^n} u^2 \, d\nu_{\mathbf{x}_0; t_0 - r^2},$$

where $L = \mathrm{Span}\{x_j - x_0\}_{j=0}^K$. If $\{\mathbf{x}_i\}_{i=0}^K$ is $(k, \alpha r)$-temporally independent and $K = k - 2$, we additionally have

$$r^4 \int_{\mathbb{R}^n} |\partial_t u|^2 \, d\nu_{\mathbf{x}_0; t_0 - r^2} \leq C(\alpha, \Lambda) \max_i \left\{ N_{\mathbf{x}_i}(8r^2) - N_{\mathbf{x}_i}(r^2/8) \right\} \int_{\mathbb{R}^n} u^2 \, d\nu_{\mathbf{x}_0; t_0 - r^2}.$$

Homogeneity at many well-separated points forces higher space-time symmetry.

Frequency detects both homogeneous polynomial behavior and space-time symmetry.

Extra symmetry emerges away from a plane of symmetry

Theorem (Quantitative dimension reduction)

If u is almost symmetric with respect to a k-plane V, then away from V it is almost symmetric in $k+1$ directions, but only at a smaller scale.

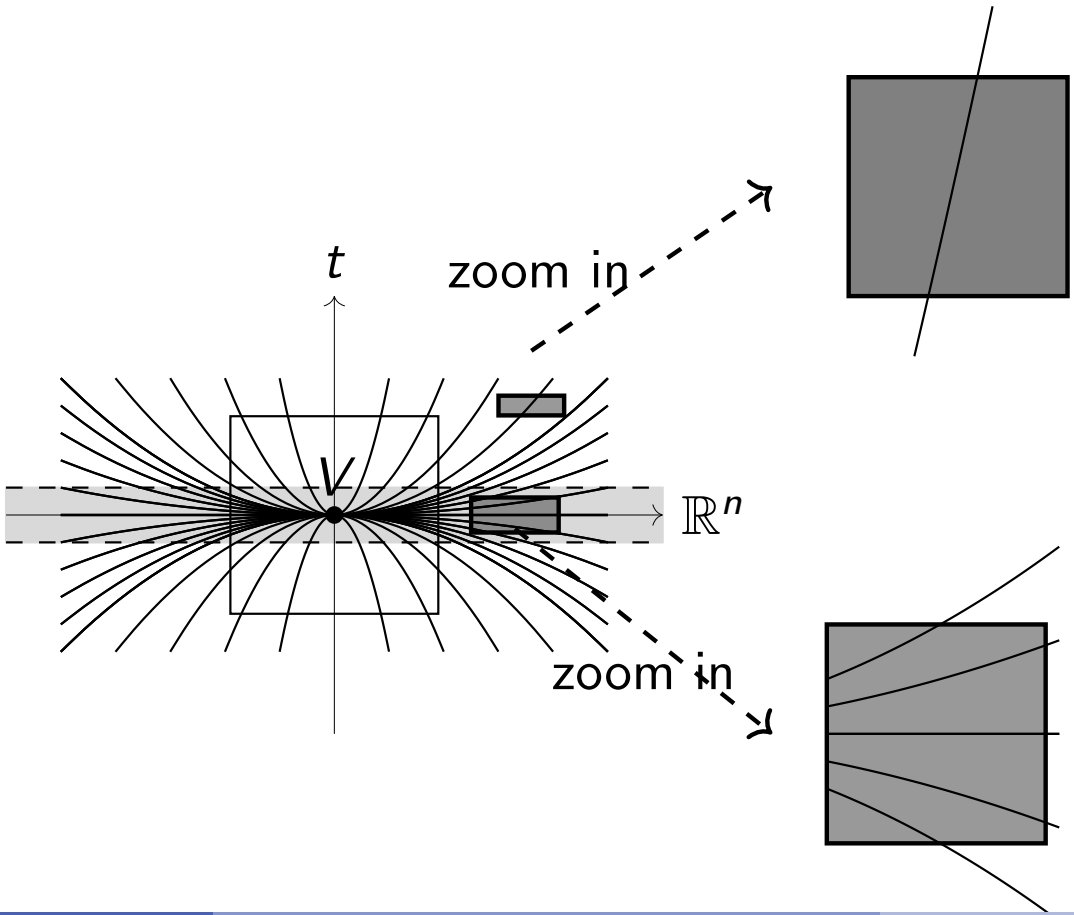

Quantitative strata and effective nodal/singular sets

All points are created symmetric, but some are more symmetric than others.

Definition (Quantitative strata)

A point lies in $\mathcal{S}^k_{\varepsilon,r}$ if it has *at most* k effective symmetries at every intermediate scale $s \in [r, 1]$.

Definition (Effective nodal and singular sets)

For $r > 0$, define

$$Z_r(u) := \left\{ \mathbf{x} \in P(\mathbf{0}, 1) : \inf_{P(\mathbf{x}, \frac{s}{16})} |u|^2 \leq \frac{1}{8} \int_{\mathbb{R}^n} |u|^2 \, d\nu_{\mathbf{x};t-s^2}, \forall s \in [r, 1], \right.$$

$$S_r(u) := \left\{ \mathbf{x} \in P(\mathbf{0}, 1) : \inf_{P(\mathbf{x}, \frac{s}{16})} \left(|u|^2 + 2s^2 |\nabla u|^2 \right) \leq \frac{1}{16} \int_{\mathbb{R}^n} |u|^2 \, d\nu_{\mathbf{x};t-s^2}, \forall s \in [r, 1]. \right.$$

$$Z(u) = \cap_{r>0} Z_r(u), \; S(u) = \cap_{r>0} S_r(u).$$

Quantitative strata and effective nodal/singular sets

All points are created symmetric, but some are more symmetric than others.

Definition (Quantitative strata)

A point lies in $\mathcal{S}^k_{\varepsilon,r}$ if it has *at most* k effective symmetries at every intermediate scale $s \in [r, 1]$.

Definition (Effective nodal and singular sets)

For $r > 0$, define

$$Z_r(u) := \left\{ \mathbf{x} \in P(\mathbf{0}, 1) : \inf_{P(\mathbf{x}, \frac{s}{16})} |u|^2 \leq \frac{1}{8} \int_{\mathbb{R}^n} |u|^2 \, d\nu_{\mathbf{x};t-s^2}, \forall s \in [r, 1], \right.$$

$$S_r(u) := \left\{ \mathbf{x} \in P(\mathbf{0}, 1) : \inf_{P(\mathbf{x}, \frac{s}{16})} \left(|u|^2 + 2s^2 |\nabla u|^2 \right) \leq \frac{1}{16} \int_{\mathbb{R}^n} |u|^2 \, d\nu_{\mathbf{x};t-s^2}, \forall s \in [r, 1]. \right.$$

$$Z(u) = \cap_{r>0} Z_r(u), \; S(u) = \cap_{r>0} S_r(u).$$

Quantitative strata and effective nodal/singular sets

All points are created symmetric, but some are more symmetric than others.

Definition (Quantitative strata)

A point lies in $\mathcal{S}^k_{\varepsilon,r}$ if it has *at most* k effective symmetries at every intermediate scale $s \in [r, 1]$.

Definition (Effective nodal and singular sets)

For $r > 0$, define

$$Z_r(u) := \left\{ \mathbf{x} \in P(\mathbf{0}, 1) : \inf_{P(\mathbf{x}, \frac{s}{16})} |u|^2 \leq \frac{1}{8} \int_{\mathbb{R}^n} |u|^2 \, d\nu_{\mathbf{x};t-s^2}, \forall s \in [r, 1], \right.$$

$$S_r(u) := \left\{ \mathbf{x} \in P(\mathbf{0}, 1) : \inf_{P(\mathbf{x}, \frac{s}{16})} \left(|u|^2 + 2s^2 |\nabla u|^2 \right) \leq \frac{1}{16} \int_{\mathbb{R}^n} |u|^2 \, d\nu_{\mathbf{x};t-s^2}, \forall s \in [r, 1]. \right.$$

$$Z(u) = \cap_{r>0} Z_r(u), \; S(u) = \cap_{r>0} S_r(u).$$

Quantitative strata and effective nodal/singular sets

All points are created symmetric, but some are more symmetric than others.

Definition (Quantitative strata)

A point lies in $\mathcal{S}^k_{\varepsilon,r}$ if it has *at most* k effective symmetries at every intermediate scale $s \in [r, 1]$.

Definition (Effective nodal and singular sets)

For $r > 0$, define

$$Z_r(u) := \left\{ \mathbf{x} \in P(\mathbf{0}, 1) : \inf_{P(\mathbf{x}, \frac{s}{16})} |u|^2 \leq \frac{1}{8} \int_{\mathbb{R}^n} |u|^2 \, d\nu_{\mathbf{x}; t-s^2}, \forall s \in [r, 1], \right.$$

$$S_r(u) := \left\{ \mathbf{x} \in P(\mathbf{0}, 1) : \inf_{P(\mathbf{x}, \frac{s}{16})} \left(|u|^2 + 2s^2 |\nabla u|^2 \right) \leq \frac{1}{16} \int_{\mathbb{R}^n} |u|^2 \, d\nu_{\mathbf{x}; t-s^2}, \forall s \in [r, 1]. \right.$$

$$Z(u) = \cap_{r>0} Z_r(u), \; S(u) = \cap_{r>0} S_r(u).$$

Quantitative strata and effective nodal/singular sets

All points are created symmetric, but some are more symmetric than others.

Definition (Quantitative strata)

A point lies in $\mathcal{S}^k_{\varepsilon,r}$ if it has *at most* k effective symmetries at every intermediate scale $s \in [r, 1]$.

Definition (Effective nodal and singular sets)

For $r > 0$, define

$$Z_r(u) := \left\{ \mathbf{x} \in P(\mathbf{0}, 1) : \inf_{P(\mathbf{x}, \frac{s}{16})} |u|^2 \leq \frac{1}{8} \int_{\mathbb{R}^n} |u|^2 \, d\nu_{\mathbf{x}; t-s^2}, \forall s \in [r, 1], \right.$$

$$S_r(u) := \left\{ \mathbf{x} \in P(\mathbf{0}, 1) : \inf_{P(\mathbf{x}, \frac{s}{16})} \left(|u|^2 + 2s^2 |\nabla u|^2 \right) \leq \frac{1}{16} \int_{\mathbb{R}^n} |u|^2 \, d\nu_{\mathbf{x}; t-s^2}, \forall s \in [r, 1]. \right.$$

$$Z(u) = \cap_{r>0} Z_r(u), \; S(u) = \cap_{r>0} S_r(u).$$

Maximal symmetry rules out nodal and singular sets

Theorem (ε-regularity)

$$Z_r(u) \subset \mathcal{S}^{n+1}_{\varepsilon,r} \qquad \text{and} \qquad S_r(u) \subset \mathcal{S}^{n}_{\varepsilon,r}.$$

The proof is an L^2 version of the rigidity argument from earlier.

- If a nonzero caloric function is symmetric in all space-time directions, then $\partial_t u = 0$, $\nabla u = 0$, so $u \equiv c \neq 0$ and hence $Z(u) = \emptyset$.
- If a caloric function is symmetric in all but one direction, then after rotation $\partial_t u = 0$, $\partial_i u = 0 \quad (1 \leq i \leq n-1)$. Thus $u = u(x_n)$ and $\Delta u = 0$, so u is linear and therefore $S(u) = \emptyset$.

Thus understanding the geometry and volume estimates for $Z_r(u)$ and $S_r(u)$ reduces to investigating quantitative strata $\mathcal{S}^k_{\varepsilon,r}$, $k \in \{n, n+1\}$.

Maximal symmetry rules out nodal and singular sets

Theorem (ε-regularity)

$$Z_r(u) \subset \mathcal{S}^{n+1}_{\varepsilon,r} \qquad \text{and} \qquad S_r(u) \subset \mathcal{S}^{n}_{\varepsilon,r}.$$

The proof is an L^2 version of the rigidity argument from earlier.

- If a nonzero caloric function is symmetric in all space-time directions, then $\partial_t u = 0$, $\nabla u = 0$, so $u \equiv c \neq 0$ and hence $Z(u) = \emptyset$.
- If a caloric function is symmetric in all but one direction, then after rotation $\partial_t u = 0$, $\partial_i u = 0 \quad (1 \leq i \leq n-1)$. Thus $u = u(x_n)$ and $\Delta u = 0$, so u is linear and therefore $S(u) = \emptyset$.

Thus understanding the geometry and volume estimates for $Z_r(u)$ and $S_r(u)$ reduces to investigating quantitative strata $\mathcal{S}^k_{\varepsilon,r}$, $k \in \{n, n+1\}$.

Maximal symmetry rules out nodal and singular sets

Theorem (ε-regularity)

$Z_r(u) \subset \mathcal{S}^{n+1}_{\varepsilon,r}$ *and* $S_r(u) \subset \mathcal{S}^{n}_{\varepsilon,r}$.

The proof is an L^2 version of the rigidity argument from earlier.

- If a nonzero caloric function is symmetric in all space-time directions, then $\partial_t u = 0$, $\nabla u = 0$, so $u \equiv c \neq 0$ and hence $Z(u) = \emptyset$.
- If a caloric function is symmetric in all but one direction, then after rotation $\partial_t u = 0$, $\partial_i u = 0 \quad (1 \leq i \leq n-1)$. Thus $u = u(x_n)$ and $\Delta u = 0$, so u is linear and therefore $S(u) = \emptyset$.

Thus understanding the geometry and volume estimates for $Z_r(u)$ and $S_r(u)$ reduces to investigating quantitative strata $\mathcal{S}^k_{\varepsilon,r}$, $k \in \{n, n+1\}$.

Maximal symmetry rules out nodal and singular sets

Theorem (ε-regularity)

$Z_r(u) \subset \mathcal{S}^{n+1}_{\varepsilon,r}$ *and* $S_r(u) \subset \mathcal{S}^{n}_{\varepsilon,r}$.

The proof is an L^2 version of the rigidity argument from earlier.

- If a nonzero caloric function is symmetric in all space-time directions, then $\partial_t u = 0$, $\nabla u = 0$, so $u \equiv c \neq 0$ and hence $Z(u) = \emptyset$.
- If a caloric function is symmetric in all but one direction, then after rotation $\partial_t u = 0$, $\partial_i u = 0 \quad (1 \leq i \leq n-1)$. Thus $u = u(x_n)$ and $\Delta u = 0$, so u is linear and therefore $S(u) = \emptyset$.

Thus understanding the geometry and volume estimates for $Z_r(u)$ and $S_r(u)$ reduces to investigating quantitative strata $\mathcal{S}^k_{\varepsilon,r}$, $k \in \{n, n+1\}$.

A telescoping estimate guarantees homogeneity on most microscopic scales

Where does symmetry come from?

Assuming $N_x(10^5) < \Lambda$, the telescoping bound

$$\sum_i \left(N_x(8^{-i}) - N_x(8^{-i-1}) \right) = N_x(1) - N_x(0) < \Lambda$$

and monotonicity of N imply that the frequency is almost constant at every point on all but a bounded number of scales.

The main goal is now to use the cone-splitting principle to organize points according to their homogeneity and number of symmetries across many scales, locations, and resolutions.

A telescoping estimate guarantees homogeneity on most microscopic scales

Where does symmetry come from?

Assuming $N_{\mathbf{x}}(10^5) < \Lambda$, the telescoping bound

$$\sum_i \left(N_{\mathbf{x}}(8^{-i}) - N_{\mathbf{x}}(8^{-i-1}) \right) = N_{\mathbf{x}}(1) - N_{\mathbf{x}}(0) < \Lambda$$

and monotonicity of N imply that the frequency is almost constant at every point on all but a bounded number of scales.

The main goal is now to use the cone-splitting principle to organize points according to their homogeneity and number of symmetries across many scales, locations, and resolutions.

A telescoping estimate guarantees homogeneity on most microscopic scales

Where does symmetry come from?

Assuming $N_{\mathbf{x}}(10^5) < \Lambda$, the telescoping bound

$$\sum_i \left(N_{\mathbf{x}}(8^{-i}) - N_{\mathbf{x}}(8^{-i-1}) \right) = N_{\mathbf{x}}(1) - N_{\mathbf{x}}(0) < \Lambda$$

and monotonicity of N imply that the frequency is almost constant at every point on all but a bounded number of scales.

The main goal is now to use the cone-splitting principle to organize points according to their homogeneity and number of symmetries across many scales, locations, and resolutions.

Neck regions organize multiscale polynomial symmetry

A k-**neck region** is, informally, a region where across *many scales* $\mathcal{S}^k_{\epsilon,r} \subset \mathcal{C}$ is quantitatively trapped near **a single** k-**plane.**

A neck region is $\mathcal{N} := P(x_0, 2r) \setminus P(\mathcal{C}, r_\bullet)$, where $P(\mathcal{C}, r_\bullet) := \bigcup_{x \in \mathcal{C}} P(x, r_x)$, $\mathcal{C}$ is a closed **center set** and $r_\bullet : \mathcal{C} \to [0, \gamma r]$ is a **scale function**

For each $x \in \mathcal{C}$ and each scale $s \in [r_x, \gamma^{-3} r]$, u has k **symmetries** with respect to a **fixed plane** V, but **does not have** $k+1$ **symmetries**.

$\mathcal{C}$ is quantitatively trapped near V, and conversely V is covered by parabolic balls centered on $\mathcal{C}$, up to the **resolution** $r_\bullet$.

Strong neck = neck + two upgrades: V is covered by balls centered on $\mathcal{C}$, and $r_\bullet$ is *parabolically* δ*-Lipschitz*.

Neck regions are where the parabolic graphs are built and the content estimates are proved.

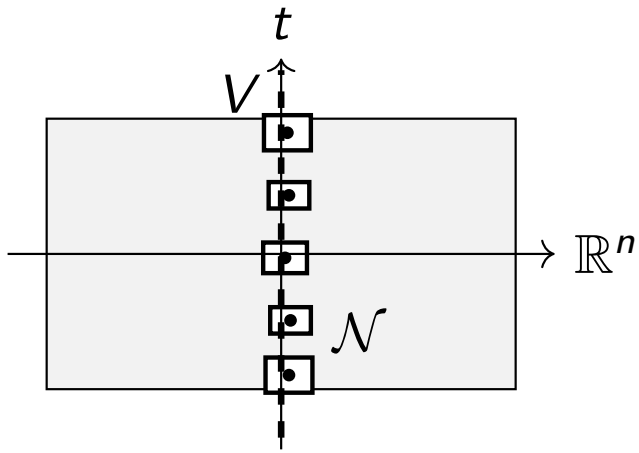

Neck regions organize multiscale polynomial symmetry

A k-**neck region** is, informally, a region where across *many scales* $\mathcal{S}^k_{\epsilon,r} \subset \mathcal{C}$ is quantitatively trapped near **a single** k-**plane.**

A neck region is $\mathcal{N} := P(x_0, 2r) \setminus P(\mathcal{C}, r_\bullet)$, where $P(\mathcal{C}, r_\bullet) := \bigcup_{x \in \mathcal{C}} P(x, r_x)$, $\mathcal{C}$ is a closed **center set** and $r_\bullet : \mathcal{C} \to [0, \gamma r]$ is a **scale function**

For each $x \in \mathcal{C}$ and each scale $s \in [r_x, \gamma^{-3} r]$, u has k **symmetries** with respect to a **fixed plane** V, but **does not have** $k+1$ **symmetries**.

$\mathcal{C}$ is quantitatively trapped near V, and conversely V is covered by parabolic balls centered on $\mathcal{C}$, up to the **resolution** $r_\bullet$.

Strong neck = neck + two upgrades: V is covered by balls centered on $\mathcal{C}$, and $r_\bullet$ is *parabolically* δ*-Lipschitz*.

Neck regions are where the parabolic graphs are built and the content estimates are proved.

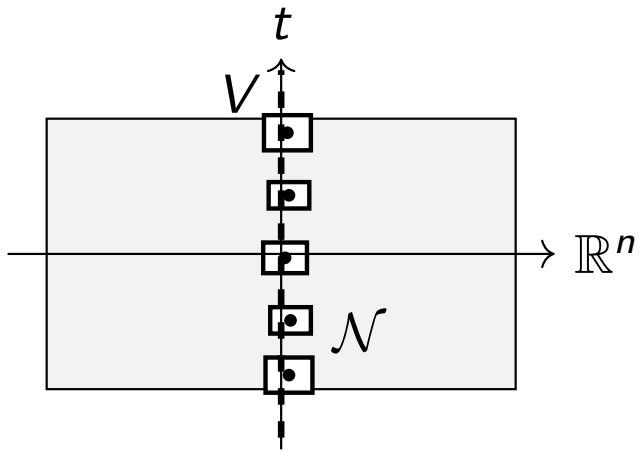

Neck regions organize multiscale polynomial symmetry

A k-**neck region** is, informally, a region where across *many scales* $\mathcal{S}^k_{\epsilon,r} \subset \mathcal{C}$ is quantitatively trapped near **a single** k-**plane.**

A neck region is $\mathcal{N} := P(x_0, 2r) \setminus P(\mathcal{C}, r_\bullet)$, where $P(\mathcal{C}, r_\bullet) := \bigcup_{x \in \mathcal{C}} P(x, r_x)$, $\mathcal{C}$ is a closed **center set** and $r_\bullet : \mathcal{C} \to [0, \gamma r]$ is a **scale function**

For each $x \in \mathcal{C}$ and each scale $s \in [r_x, \gamma^{-3} r]$, u has k **symmetries** with respect to a **fixed plane** V, but **does not have** $k+1$ **symmetries**.

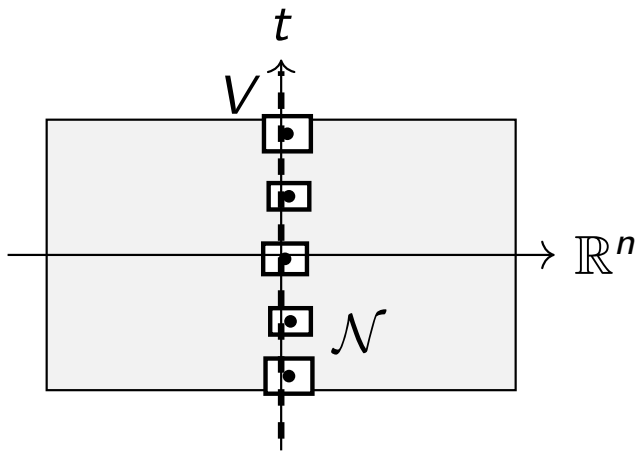

$\mathcal{C}$ is quantitatively trapped near V, and conversely V is covered by parabolic balls centered on $\mathcal{C}$, up to the **resolution** $r_\bullet$.

Strong neck = neck + two upgrades: V is covered by balls centered on $\mathcal{C}$, and $r_\bullet$ is *parabolically* δ*-Lipschitz*.

Neck regions are where the parabolic graphs are built and the content estimates are proved.

Neck regions organize multiscale polynomial symmetry

A k-**neck region** is, informally, a region where across *many scales* $\mathcal{S}^k_{\epsilon,r} \subset \mathcal{C}$ is quantitatively trapped near **a single** k-**plane.**

A neck region is $\mathcal{N} := P(x_0, 2r) \setminus P(\mathcal{C}, r_\bullet)$, where $P(\mathcal{C}, r_\bullet) := \bigcup_{x \in \mathcal{C}} P(x, r_x)$, $\mathcal{C}$ is a closed **center set** and $r_\bullet : \mathcal{C} \to [0, \gamma r]$ is a **scale function**

For each $x \in \mathcal{C}$ and each scale $s \in [r_x, \gamma^{-3} r]$, u has k **symmetries** with respect to a **fixed plane** V, but **does not have** $k+1$ **symmetries**.

$\mathcal{C}$ is quantitatively trapped near V, and conversely V is covered by parabolic balls centered on $\mathcal{C}$, up to the **resolution** $r_\bullet$.

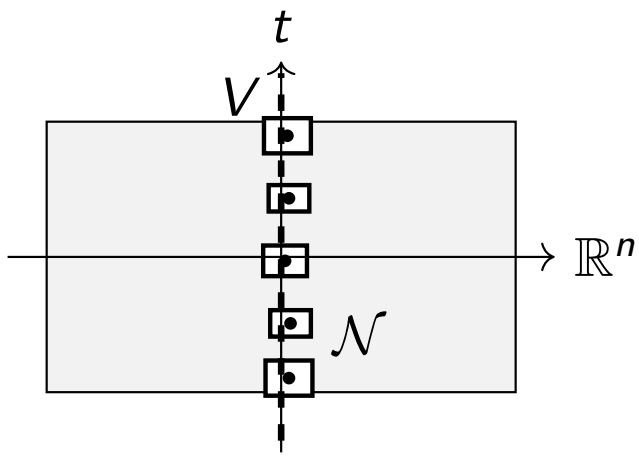

Strong neck = neck + two upgrades: V is covered by balls centered on $\mathcal{C}$, and $r_\bullet$ is *parabolically* δ*-Lipschitz.*

Neck regions are where the parabolic graphs are built and the content estimates are proved.

Neck regions organize multiscale polynomial symmetry

A k-**neck region** is, informally, a region where across *many scales* $\mathcal{S}^k_{\epsilon,r} \subset \mathcal{C}$ is quantitatively trapped near **a single** k-**plane.**

A neck region is $\mathcal{N} := P(x_0, 2r) \setminus P(\mathcal{C}, r_\bullet)$, where $P(\mathcal{C}, r_\bullet) := \bigcup_{x \in \mathcal{C}} P(x, r_x)$, $\mathcal{C}$ is a closed **center set** and $r_\bullet : \mathcal{C} \to [0, \gamma r]$ is a **scale function**

For each $x \in \mathcal{C}$ and each scale $s \in [r_x, \gamma^{-3} r]$, u has k **symmetries** with respect to a **fixed plane** V, but **does not have** $k+1$ **symmetries**.

$\mathcal{C}$ is quantitatively trapped near V, and conversely V is covered by parabolic balls centered on $\mathcal{C}$, up to the **resolution** $r_\bullet$.

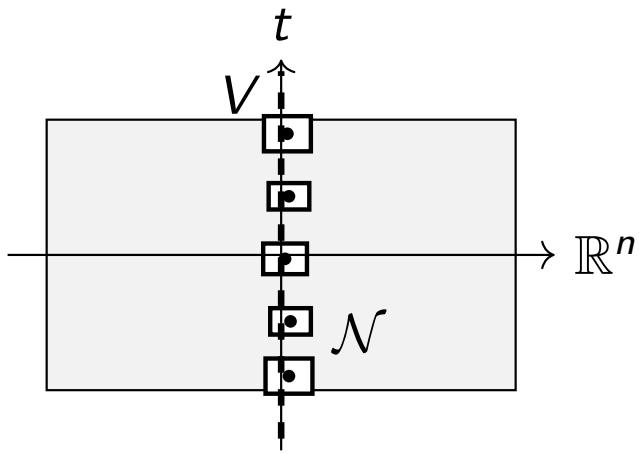

Strong neck = neck + two upgrades: V is covered by balls centered on $\mathcal{C}$, and $r_\bullet$ is *parabolically* δ*-Lipschitz*.

Neck regions are where the parabolic graphs are built and the content estimates are proved.

Neck regions organize multiscale polynomial symmetry

A k-**neck region** is, informally, a region where across *many scales* $\mathcal{S}^k_{\epsilon,r} \subset \mathcal{C}$ is quantitatively trapped near **a single** k-**plane.**

A neck region is $\mathcal{N} := P(x_0, 2r) \setminus P(\mathcal{C}, r_\bullet)$, where $P(\mathcal{C}, r_\bullet) := \bigcup_{x \in \mathcal{C}} P(x, r_x)$, $\mathcal{C}$ is a closed **center set** and $r_\bullet : \mathcal{C} \to [0, \gamma r]$ is a **scale function**

For each $x \in \mathcal{C}$ and each scale $s \in [r_x, \gamma^{-3} r]$, u has k **symmetries** with respect to a **fixed plane** V, but **does not have** $k+1$ **symmetries**.

$\mathcal{C}$ is quantitatively trapped near V, and conversely V is covered by parabolic balls centered on $\mathcal{C}$, up to the **resolution** $r_\bullet$.

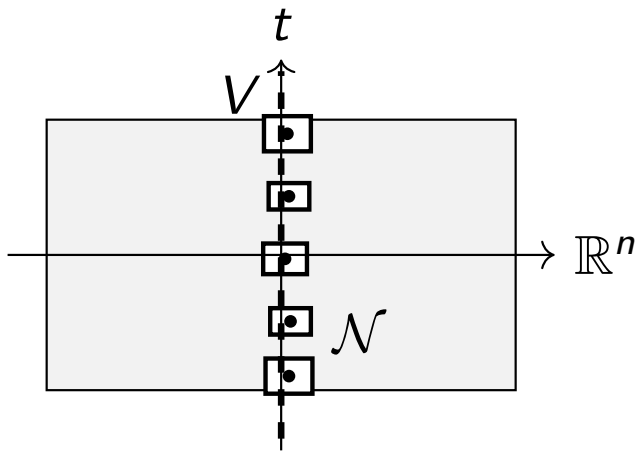

Strong neck = neck + two upgrades: V is covered by balls centered on $\mathcal{C}$, and $r_\bullet$ is *parabolically* δ*-Lipschitz*.

Neck regions are where the parabolic graphs are built and the content estimates are proved.

Neck structure theorem I

Neck structure theorem: multiscale trapping near the plane V implies packing content estimate for $\mathcal{C}$ and for $\mathcal{S}^k_{\epsilon,r}$.

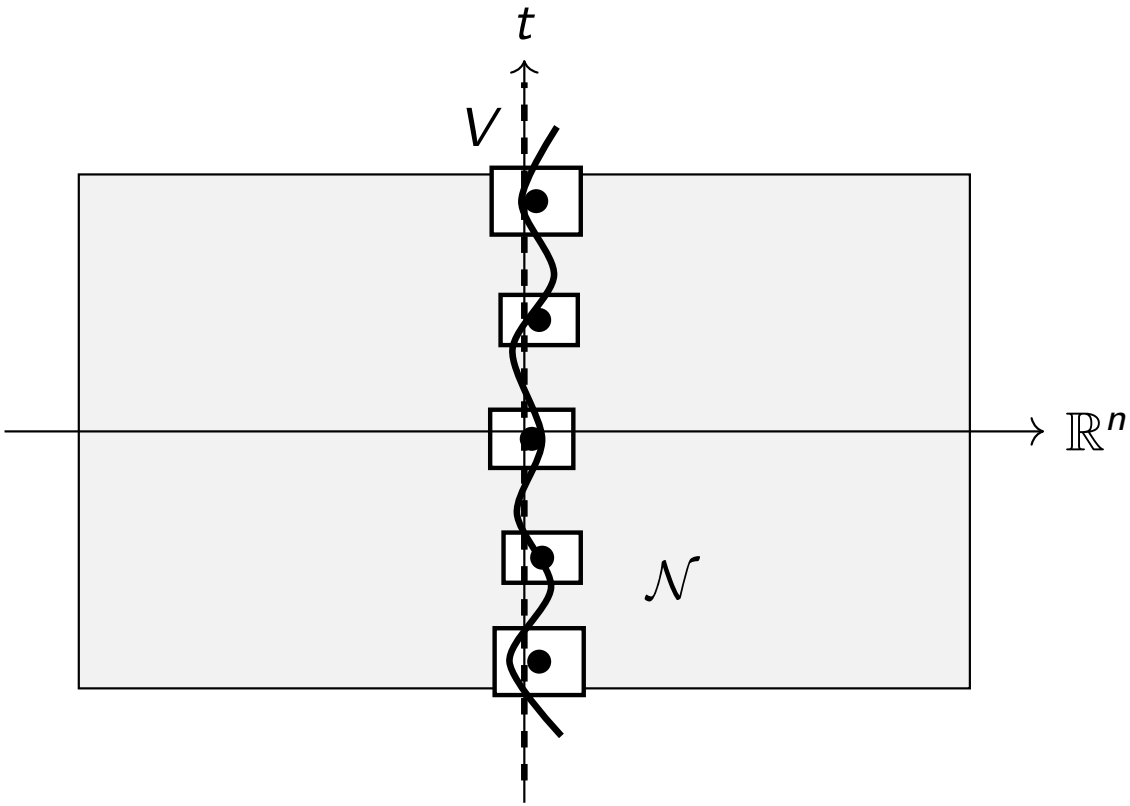

$$P(x_0, 2r) = B(x_0, 2r) \times (t_0 \pm (2r)^2)$$

Regular parabolic Lipschitz graphs

Fix a vertical k-plane V and write a graph $\Gamma = \{y + G(y) : y \in V\}$ with $G : V \to V^{\perp}$.

Parabolic Lipschitz: $|G(y) - G(z)| \leq \delta\, |y - z|_{\mathcal{P}} \qquad (y, z \in V).$

Half-time derivative: define for compactly supported φ

$$\partial_t^{1/2} \varphi(x,t) := c \int_{\mathbb{R}} \frac{\varphi(x,s) - \varphi(x,t)}{|s-t|^{3/2}}\, ds,$$

Regularity condition: $\partial_t^{1/2} G$ has *parabolic BMO* control on V:

$$\|\partial_t^{1/2} G\|_{\mathrm{BMO}_{\mathcal{P}}(V)} \lesssim \delta.$$

Regular parabolic Lipschitz graphs

Fix a vertical k-plane V and write a graph $\Gamma = \{y + G(y) : y \in V\}$ with $G : V \to V^{\perp}$.

Parabolic Lipschitz: $|G(y) - G(z)| \leq \delta\, |y - z|_{\mathcal{P}} \qquad (y, z \in V).$

Half-time derivative: define for compactly supported φ

$$\partial_t^{1/2} \varphi(x,t) := c \int_{\mathbb{R}} \frac{\varphi(x,s) - \varphi(x,t)}{|s-t|^{3/2}}\, ds,$$

Regularity condition: $\partial_t^{1/2} G$ has *parabolic BMO* control on V:

$$\|\partial_t^{1/2} G\|_{\mathrm{BMO}_{\mathcal{P}}(V)} \lesssim \delta.$$

Regular parabolic Lipschitz graphs

Fix a vertical k-plane V and write a graph $\Gamma = \{y + G(y) : y \in V\}$ with $G : V \to V^{\perp}$.

Parabolic Lipschitz: $|G(y) - G(z)| \leq \delta\, |y - z|_{\mathcal{P}} \qquad (y, z \in V).$

Half-time derivative: define for compactly supported φ

$$\partial_t^{1/2}\varphi(x,t) := c \int_{\mathbb{R}} \frac{\varphi(x,s) - \varphi(x,t)}{|s-t|^{3/2}}\, ds,$$

Regularity condition: $\partial_t^{1/2} G$ has *parabolic BMO* control on V:

$$\|\partial_t^{1/2} G\|_{\mathrm{BMO}_{\mathcal{P}}(V)} \lesssim \delta.$$

Regular parabolic Lipschitz graphs

Fix a vertical k-plane V and write a graph $\Gamma = \{y + G(y) : y \in V\}$ with $G : V \to V^{\perp}$.

Parabolic Lipschitz: $|G(y) - G(z)| \leq \delta\, |y - z|_{\mathcal{P}} \qquad (y, z \in V).$

Half-time derivative: define for compactly supported φ

$$\partial_t^{1/2}\varphi(x,t) := c \int_{\mathbb{R}} \frac{\varphi(x,s) - \varphi(x,t)}{|s-t|^{3/2}}\, ds,$$

Regularity condition: $\partial_t^{1/2} G$ has *parabolic BMO* control on V:

$\|\partial_t^{1/2} G\|_{\mathrm{BMO}_P(V)} \lesssim \delta.$

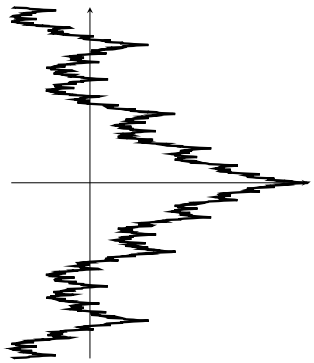

Strong multiscale trapping forces regular graphicality

Theorem (Strong neck structure theorem)

Assume $k \in \{n,\ n{+}1\}$ and $\mathcal{N} = P(x_0, 2r) \setminus P(\mathcal{C}, r_\bullet)$ is a **strong** *(m, k, δ, η)-neck region modeled on a vertical plane V. Then there exists a compactly supported $C\,\delta^{1/(k+2)}$-regular parabolic Lipschitz map $G : V \to V^\perp$ such that*

$$d_P\big(x,\ \mathrm{graph}(G)\big)\ \leq\ C(\eta, \Lambda)\,\delta\, r_x \qquad \text{for all } x \in \mathcal{C} \cap P(\mathbf{x}_0, \tfrac{4}{3} r).$$

Multiscale trapping near the *vertical* plane V upgrades to a single regular parabolic $\mathrm{graph}(G)$ approximating $\mathcal{C}$.

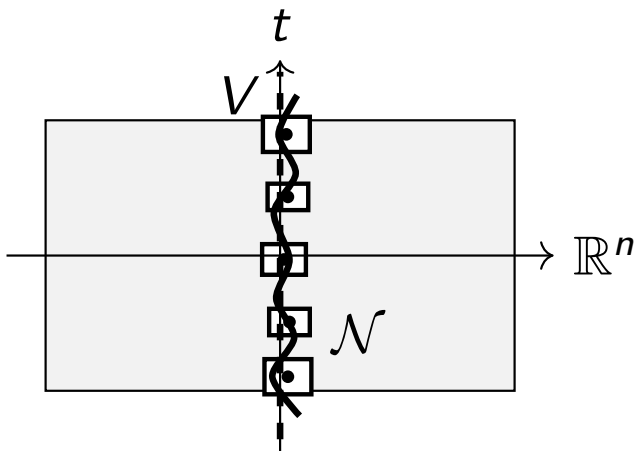

Carleson estimate for κ-number implies BMO

$$\beta^2_{\mathcal{P},k}(\mathbf{x},r) := \inf_{V\in \mathrm{Aff}_{\mathcal{P}}(k)} \frac{1}{r^k}\int_{P(\mathbf{x},r)} \left(\frac{d_{\mathcal{P}}(\mathbf{y},V)}{r}\right)^2 d\mu(\mathbf{y}).$$

In **elliptic Reifenberg theory, Carleson control of β-numbers** with respect to the packing measure μ of $\mathcal{C}$

$$\int_{B(x,10r)}\int_{\frac{1}{8}\mathbf{r}_y}^{r} \beta_k^2(y,10^5 s)\,\frac{ds}{s}\,d\mu(y) \le C\delta r^k.$$

yields a **Euclidean Lipschitz parameterization of $\mathcal{C}$.**

We need a *parabolic* Lipschitz graph with $\partial_t^{1/2}$-BMO control. Upgrade β-control to a **Carleson estimate for a stronger "κ-number" that implies BMO for $\partial_t^{1/2}$.**

$$\kappa^2(\mathbf{x},r) := \kappa_k^2(\mathbf{x},r;G) := \inf_{\ell} \frac{1}{r^k}\int_{P(\mathbf{x},r)\cap V} \left(\frac{|G(\mathbf{y})-\ell(\mathbf{y})|}{r}\right)^2 d\mathcal{H}^k_{\mathcal{P}}(\mathbf{y}),$$

where inf is over all affine functions $\ell\colon V\to\mathbb{R}^{n+2-k}$ satisfying $\partial_t\ell\equiv 0$.

Carleson estimate for κ-number implies BMO

$$\beta^2_{\mathcal{P},k}(\mathbf{x},r) := \inf_{V\in \mathrm{Aff}_{\mathcal{P}}(k)} \frac{1}{r^k}\int_{P(\mathbf{x},r)} \left(\frac{d_{\mathcal{P}}(\mathbf{y},V)}{r}\right)^2 d\mu(\mathbf{y}).$$

In **elliptic Reifenberg theory, Carleson control of β-numbers** with respect to the packing measure μ of $\mathcal{C}$

$$\int_{B(x,10r)}\int_{\frac{1}{8}\mathbf{r}_y}^{r} \beta^2_k(y,10^5 s)\,\frac{ds}{s}\,d\mu(y) \le C\delta r^k.$$

yields a **Euclidean Lipschitz parameterization of $\mathcal{C}$.**

We need a *parabolic* Lipschitz graph with $\partial_t^{1/2}$-BMO control. Upgrade β-control to a **Carleson estimate for a stronger "κ-number" that implies BMO for $\partial_t^{1/2}$.**

$$\kappa^2(\mathbf{x},r) := \kappa^2_k(\mathbf{x},r;G) := \inf_{\ell} \frac{1}{r^k}\int_{P(\mathbf{x},r)\cap V} \left(\frac{|G(\mathbf{y})-\ell(\mathbf{y})|}{r}\right)^2 d\mathcal{H}^k_{\mathcal{P}}(\mathbf{y}),$$

where inf is over all affine functions $\ell\colon V\to\mathbb{R}^{n+2-k}$ satisfying $\partial_t\ell\equiv 0$.

Carleson estimate for κ-number implies BMO

$$\beta^2_{\mathcal{P},k}(\mathbf{x},r) := \inf_{V\in \mathrm{Aff}_{\mathcal{P}}(k)} \frac{1}{r^k}\int_{P(\mathbf{x},r)} \left(\frac{d_{\mathcal{P}}(\mathbf{y},V)}{r}\right)^2 d\mu(\mathbf{y}).$$

In **elliptic Reifenberg theory, Carleson control of β-numbers** with respect to the packing measure μ of $\mathcal{C}$

$$\int_{B(x,10r)}\int_{\frac{1}{8}\mathbf{r}_y}^{r} \beta^2_k(y,10^5 s)\,\frac{ds}{s}\,d\mu(y) \le C\delta r^k.$$

yields a **Euclidean Lipschitz parameterization of $\mathcal{C}$.**

We need a *parabolic* Lipschitz graph with $\partial_t^{1/2}$-BMO control. Upgrade β-control to a **Carleson estimate for a stronger "κ-number" that implies BMO for $\partial_t^{1/2}$.**

$$\kappa^2(\mathbf{x},r) := \kappa^2_k(\mathbf{x},r;G) := \inf_{\ell} \frac{1}{r^k}\int_{P(\mathbf{x},r)\cap V} \left(\frac{|G(\mathbf{y})-\ell(\mathbf{y})|}{r}\right)^2 d\mathcal{H}^k_{\mathcal{P}}(\mathbf{y}),$$

where inf is over all affine functions $\ell\colon V\to\mathbb{R}^{n+2-k}$ satisfying $\partial_t\ell\equiv 0$.

Carleson estimate for κ-number implies BMO

$$\beta^2_{\mathcal{P},k}(\mathbf{x},r) := \inf_{V\in \mathrm{Aff}_{\mathcal{P}}(k)} \frac{1}{r^k}\int_{P(\mathbf{x},r)} \left(\frac{d_{\mathcal{P}}(\mathbf{y},V)}{r}\right)^2 d\mu(\mathbf{y}).$$

In **elliptic Reifenberg theory, Carleson control of β-numbers** with respect to the packing measure μ of $\mathcal{C}$

$$\int_{B(x,10r)}\int_{\frac{1}{8}\mathbf{r}_y}^{r} \beta^2_k(y,10^5 s)\,\frac{ds}{s}\,d\mu(y) \le C\delta r^k.$$

yields a **Euclidean Lipschitz parameterization of $\mathcal{C}$.**

We need a *parabolic* Lipschitz graph with $\partial_t^{1/2}$-BMO control. Upgrade β-control to a **Carleson estimate for a stronger "κ-number" that implies BMO for $\partial_t^{1/2}$.**

$$\kappa^2(\mathbf{x},r) := \kappa^2_k(\mathbf{x},r;G) := \inf_{\ell} \frac{1}{r^k}\int_{P(\mathbf{x},r)\cap V} \left(\frac{|G(\mathbf{y})-\ell(\mathbf{y})|}{r}\right)^2 d\mathcal{H}^k_{\mathcal{P}}(\mathbf{y}),$$

where inf is over all affine functions $\ell\colon V\to\mathbb{R}^{n+2-k}$ satisfying $\partial_t\ell\equiv 0$.

Local tangents quantitatively align along V

On a **strong vertical neck,** every $\mathbf{x} \in \mathcal{C}$ has a **best vertical k-plane** $V_{\mathbf{x}}(s)$ at each scale $s \in [r_x, \gamma^{-3} r]$ (from (k, δ, s)-symmetry).

Step 1: $V_{\mathbf{x}}(s)$ is a good tangent approximation: $\mathcal{C} \cap P(\mathbf{x}, s) \subset P(\mathbf{x} + V_{\mathbf{x}}(s), \delta s)$ and $(\mathbf{x} + V_{\mathbf{x}}(s)) \cap P(\mathbf{x}, s) \subset P(\mathcal{C}, \gamma s)$.

Step 2: $V_{\mathbf{x}}(s)$ are coherent across scales:

$$\angle(V_{\mathbf{x}}(s), V_{\mathbf{x}}(2s)) \lesssim \beta(\mathbf{x}, s),$$

Step 3: All $V_{\mathbf{x}}(s)$ stay close to a single vertical plane V on $\mathcal{N}$.

Local tangents align along one global plane V.

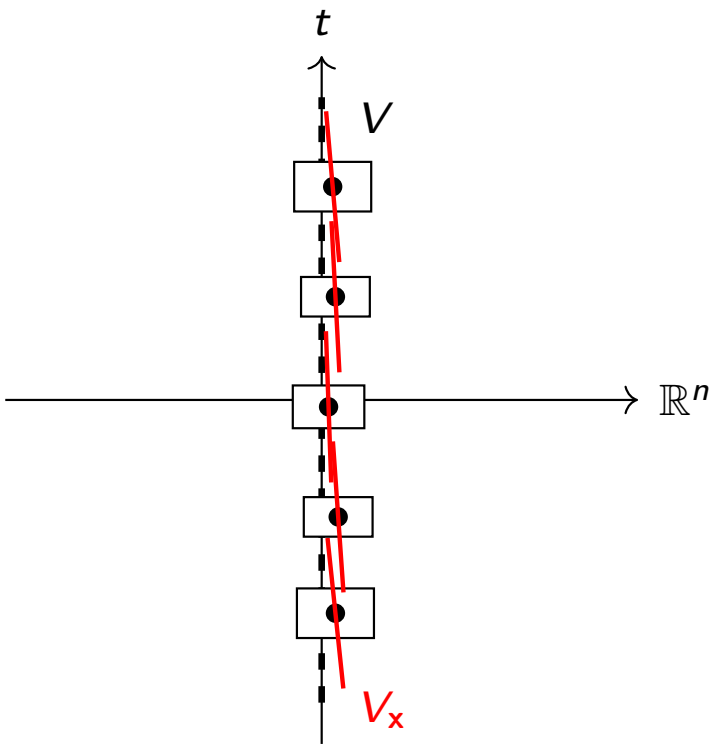

Warning for fig: All $V_{\mathbf{x}}$ are vertical. Tilting is happening in space.

Local tangents quantitatively align along V

On a **strong vertical neck,** every $\mathbf{x} \in \mathcal{C}$ has a **best vertical k-plane** $V_{\mathbf{x}}(s)$ at each scale $s \in [r_x, \gamma^{-3} r]$ (from (k, δ, s)-symmetry).

Step 1: $V_{\mathbf{x}}(s)$ is a good tangent approximation: $\mathcal{C} \cap P(\mathbf{x}, s) \subset P(\mathbf{x} + V_{\mathbf{x}}(s), \delta s)$ and $(\mathbf{x} + V_{\mathbf{x}}(s)) \cap P(\mathbf{x}, s) \subset P(\mathcal{C}, \gamma s)$.

Step 2: $V_{\mathbf{x}}(s)$ are coherent across scales:

$$\angle(V_{\mathbf{x}}(s), V_{\mathbf{x}}(2s)) \lesssim \beta(\mathbf{x}, s),$$

Step 3: All $V_{\mathbf{x}}(s)$ stay close to a single vertical plane V on $\mathcal{N}$.

Local tangents align along one global plane V.

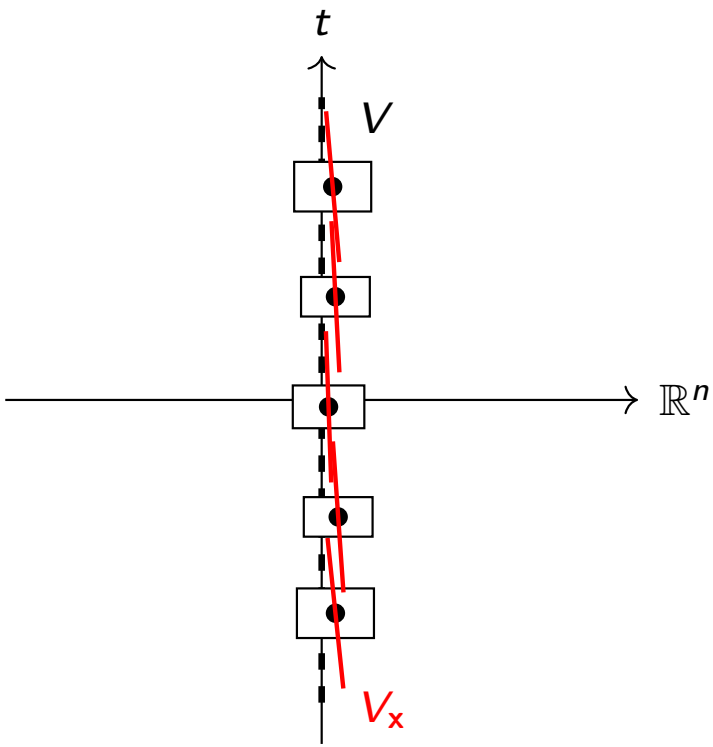

Warning for fig: All $V_{\mathbf{x}}$ are vertical. Tilting is happening in space.

Local tangents quantitatively align along V

On a **strong vertical neck,** every $\mathbf{x} \in \mathcal{C}$ has a **best vertical k-plane** $V_{\mathbf{x}}(s)$ at each scale $s \in [r_x, \gamma^{-3} r]$ (from (k, δ, s)-symmetry).

Step 1: $V_{\mathbf{x}}(s)$ is a good tangent approximation: $\mathcal{C} \cap P(\mathbf{x}, s) \subset P(\mathbf{x} + V_{\mathbf{x}}(s), \delta s)$ and $(\mathbf{x} + V_{\mathbf{x}}(s)) \cap P(\mathbf{x}, s) \subset P(\mathcal{C}, \gamma s)$.

Step 2: $V_{\mathbf{x}}(s)$ are coherent across scales:

$$\angle(V_{\mathbf{x}}(s), V_{\mathbf{x}}(2s)) \lesssim \beta(\mathbf{x}, s),$$

Step 3: All $V_{\mathbf{x}}(s)$ stay close to a single vertical plane V on $\mathcal{N}$.

Local tangents align along one global plane V.

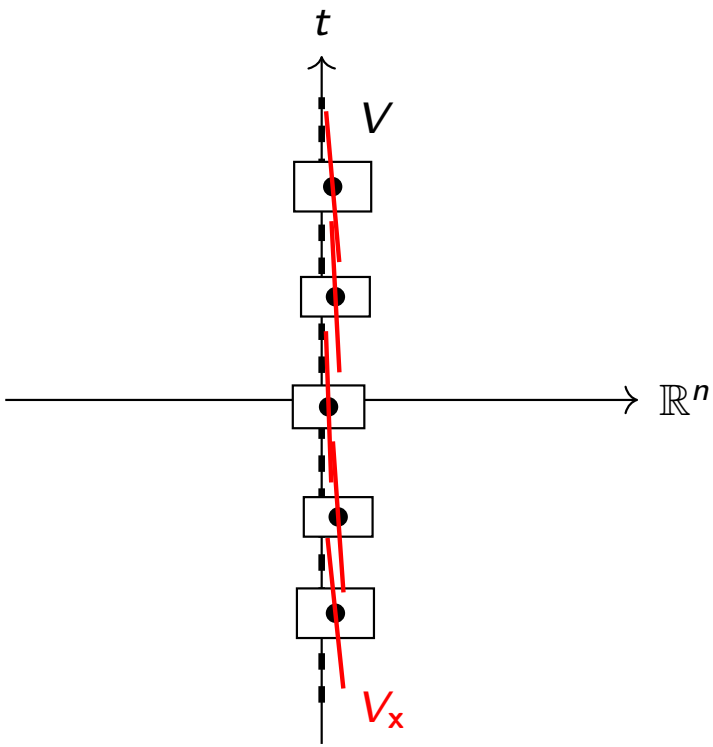

Warning for fig: All $V_{\mathbf{x}}$ are vertical. Tilting is happening in space.

Local tangents quantitatively align along V

On a **strong vertical neck,** every $\mathbf{x} \in \mathcal{C}$ has a **best vertical k-plane** $V_{\mathbf{x}}(s)$ at each scale $s \in [r_x, \gamma^{-3} r]$ (from (k, δ, s)-symmetry).

Step 1: $V_{\mathbf{x}}(s)$ is a good tangent approximation: $\mathcal{C} \cap P(\mathbf{x}, s) \subset P(\mathbf{x} + V_{\mathbf{x}}(s), \delta s)$ and $(\mathbf{x} + V_{\mathbf{x}}(s)) \cap P(\mathbf{x}, s) \subset P(\mathcal{C}, \gamma s)$.

Step 2: $V_{\mathbf{x}}(s)$ are coherent across scales:

$$\angle(V_{\mathbf{x}}(s), V_{\mathbf{x}}(2s)) \lesssim \beta(\mathbf{x}, s),$$

Step 3: All $V_{\mathbf{x}}(s)$ stay close to a single vertical plane V on $\mathcal{N}$.

Local tangents align along one global plane V.

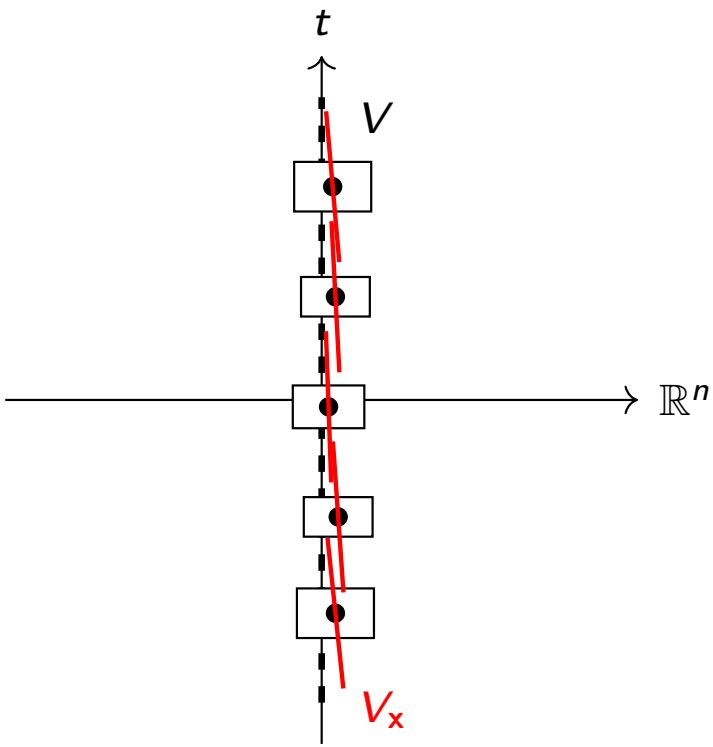

Warning for fig: All $V_{\mathbf{x}}$ are vertical. Tilting is happening in space.

Local tangents quantitatively align along V

On a **strong vertical neck,** every $\mathbf{x} \in \mathcal{C}$ has a **best vertical k-plane $V_{\mathbf{x}}(s)$** at each scale $s \in [r_x, \gamma^{-3} r]$ (from (k, δ, s)-symmetry).

Step 1: $V_{\mathbf{x}}(s)$ is a good tangent approximation: $\mathcal{C} \cap P(\mathbf{x}, s) \subset P(\mathbf{x} + V_{\mathbf{x}}(s), \delta s)$ and $(\mathbf{x} + V_{\mathbf{x}}(s)) \cap P(\mathbf{x}, s) \subset P(\mathcal{C}, \gamma s)$.

Step 2: $V_{\mathbf{x}}(s)$ are coherent across scales:

$$\angle(V_{\mathbf{x}}(s), V_{\mathbf{x}}(2s)) \lesssim \beta(\mathbf{x}, s),$$

Step 3: All $V_{\mathbf{x}}(s)$ stay close to a single vertical plane V on $\mathcal{N}$.

Local tangents align along one global plane V.

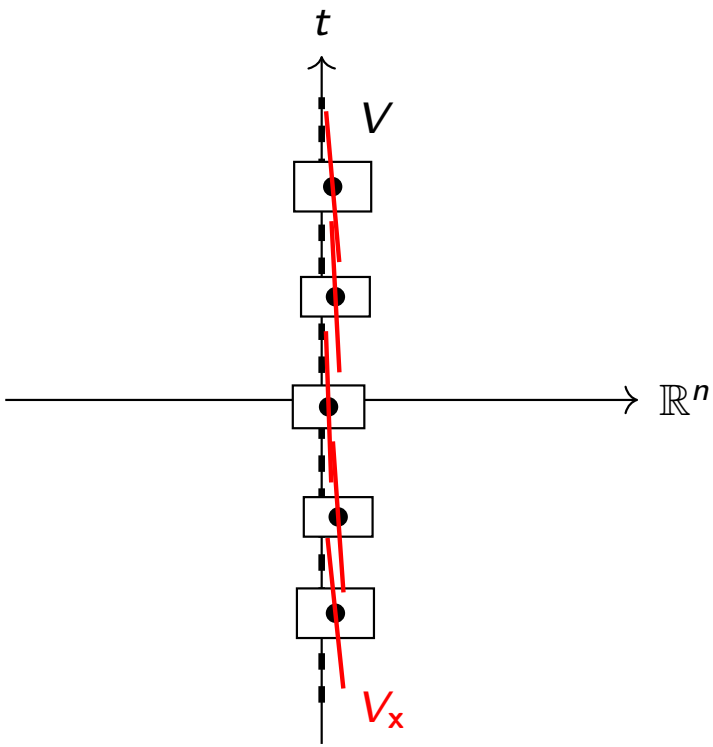

Warning for fig: All $V_{\mathbf{x}}$ are vertical. Tilting is happening in space.

Local tangents glue to form a graph with Carleson estimate

Whitney decomposition. Cover $V \cap P(\mathbf{0}, 1)$ by parabolic balls $\{P(\mathbf{y}, \mathbf{r_y})\}$ where $\mathbf{y}$ is $\mathcal{C}_+$ projected to V.

Local graph pieces. On each $P(\mathbf{y}, c\mathbf{r_y})$ choose a best k-plane $V_\mathbf{y}$ and write a local graph map $G_\mathbf{y}$ whose graph tracks $\mathcal{C}$ there.

Glue with a partition of unity. With $\{\phi_\mathbf{y}\}$ subordinate to $\{P(\mathbf{y}, \mathbf{r_y})\}$.

$$G := \sum_{\mathbf{y}} \phi_\mathbf{y} \, G_\mathbf{y}.$$

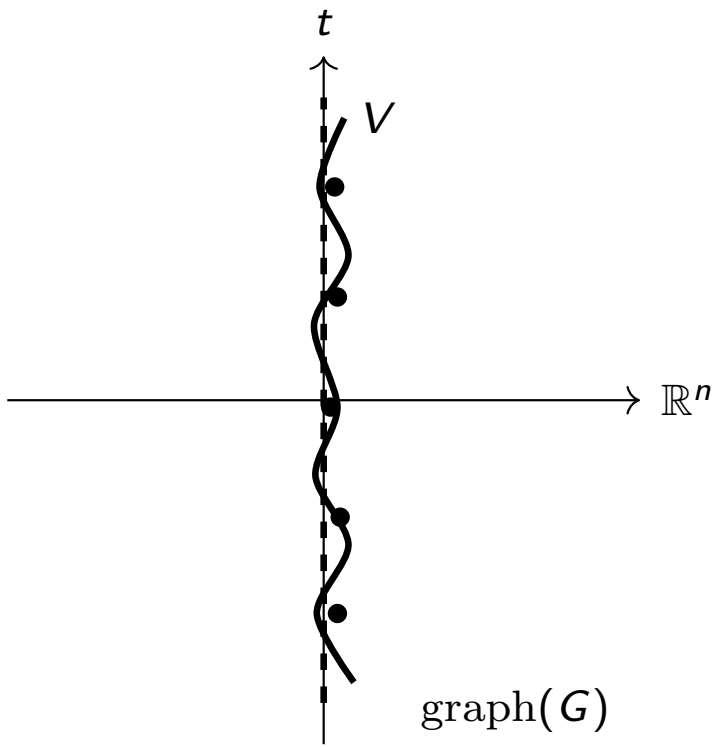

Parabolic refinement. A Carleson estimate for κ yields $\|\partial_t^{1/2} G\|_{\mathrm{BMO}_P} \lesssim$ (small), **so G is regular parabolic Lipschitz**.

For $k \in \{n, n+1\}$, $\mathcal{S}^k_{\epsilon,r}$ on a *strong* neck region is contained in a regular parabolic Lipschitz graph.

Local tangents glue to form a graph with Carleson estimate

Whitney decomposition. Cover $V \cap P(\mathbf{0}, 1)$ by parabolic balls $\{P(\mathbf{y}, \mathbf{r_y})\}$ where $\mathbf{y}$ is $\mathcal{C}_+$ projected to V.

Local graph pieces. On each $P(\mathbf{y}, c\mathbf{r_y})$ choose a best k-plane $V_\mathbf{y}$ and write a local graph map $G_\mathbf{y}$ whose graph tracks $\mathcal{C}$ there.

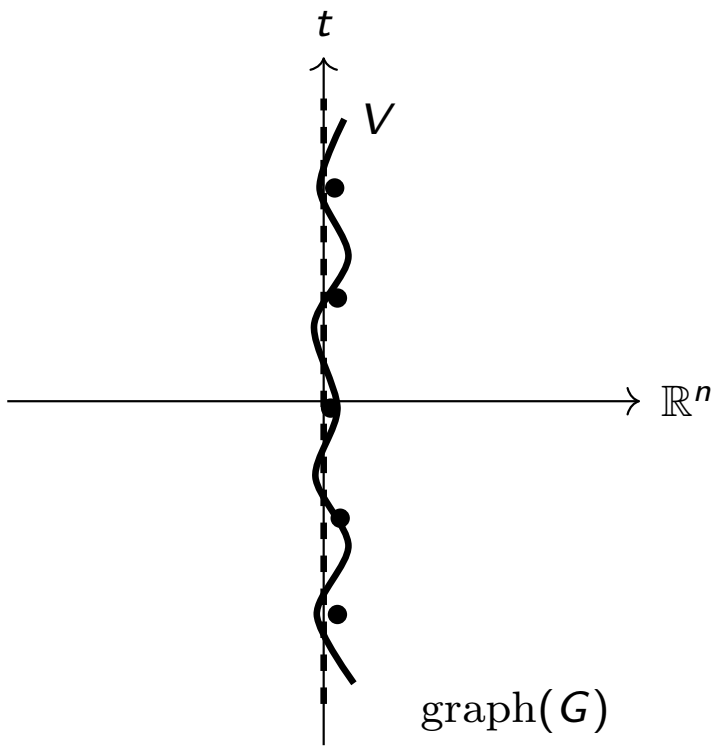

Glue with a partition of unity. With $\{\phi_\mathbf{y}\}$ subordinate to $\{P(\mathbf{y}, \mathbf{r_y})\}$.

$$G := \sum_{\mathbf{y}} \phi_\mathbf{y} \, G_\mathbf{y}.$$

Parabolic refinement. A Carleson estimate for κ yields $\|\partial_t^{1/2} G\|_{\mathrm{BMO}_P} \lesssim$ (small), **so G is regular parabolic Lipschitz**.

For $k \in \{n, n+1\}$, $\mathcal{S}^k_{\epsilon,r}$ on a *strong* neck region is contained in a regular parabolic Lipschitz graph.

Local tangents glue to form a graph with Carleson estimate

Whitney decomposition. Cover $V \cap P(\mathbf{0}, 1)$ by parabolic balls $\{P(\mathbf{y}, \mathbf{r_y})\}$ where $\mathbf{y}$ is $\mathcal{C}_+$ projected to V.

Local graph pieces. On each $P(\mathbf{y}, c\mathbf{r_y})$ choose a best k-plane $V_\mathbf{y}$ and write a local graph map $G_\mathbf{y}$ whose graph tracks $\mathcal{C}$ there.

Glue with a partition of unity. With $\{\phi_\mathbf{y}\}$ subordinate to $\{P(\mathbf{y}, \mathbf{r_y})\}$.

$$G := \sum_{\mathbf{y}} \phi_\mathbf{y} \, G_\mathbf{y}.$$

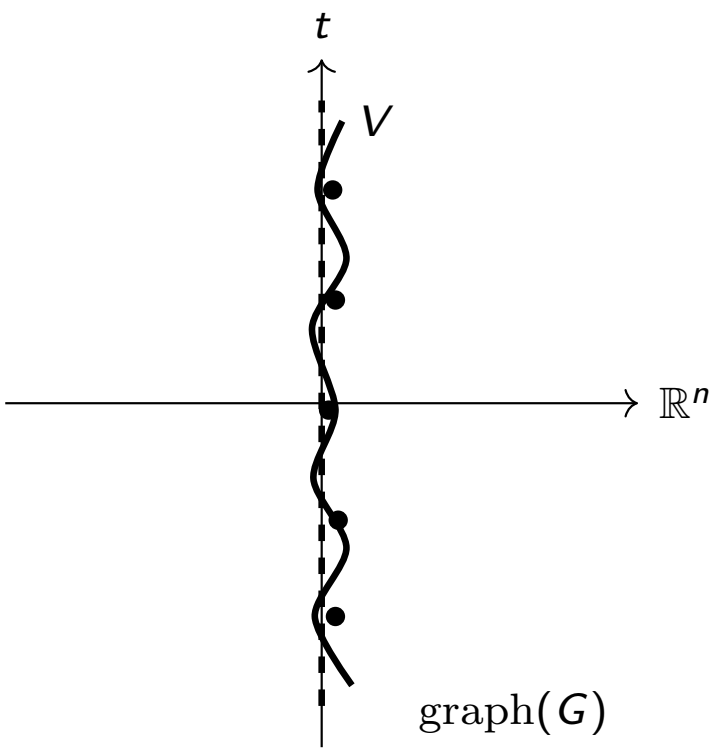

Parabolic refinement. A Carleson estimate for κ yields $\|\partial_t^{1/2} G\|_{\mathrm{BMO}_P} \lesssim$ (small), **so G is regular parabolic Lipschitz**.

For $k \in \{n, n+1\}$, $\mathcal{S}^k_{\epsilon,r}$ on a *strong* neck region is contained in a regular parabolic Lipschitz graph.

Local tangents glue to form a graph with Carleson estimate

Whitney decomposition. Cover $V \cap P(\mathbf{0}, 1)$ by parabolic balls $\{P(\mathbf{y}, \mathbf{r_y})\}$ where $\mathbf{y}$ is $\mathcal{C}_+$ projected to V.

Local graph pieces. On each $P(\mathbf{y}, c\mathbf{r_y})$ choose a best k-plane $V_\mathbf{y}$ and write a local graph map $G_\mathbf{y}$ whose graph tracks $\mathcal{C}$ there.

Glue with a partition of unity. With $\{\phi_\mathbf{y}\}$ subordinate to $\{P(\mathbf{y}, \mathbf{r_y})\}$.

$$G := \sum_{\mathbf{y}} \phi_\mathbf{y} \, G_\mathbf{y}.$$

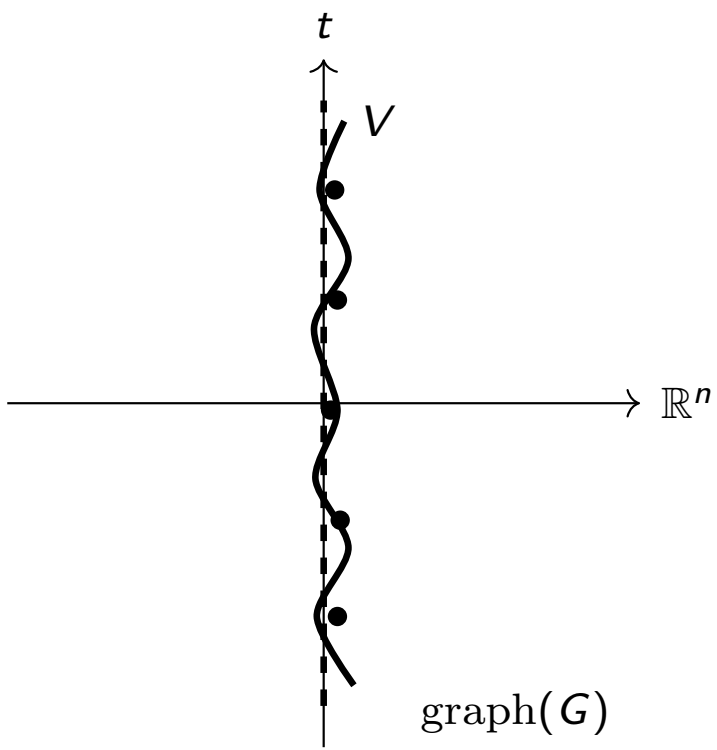

Parabolic refinement. A Carleson estimate for κ yields $\|\partial_t^{1/2} G\|_{\mathrm{BMO}_P} \lesssim$ (small), **so G is regular parabolic Lipschitz**.

For $k \in \{n, n+1\}$, $\mathcal{S}^k_{\epsilon,r}$ on a *strong* neck region is contained in a regular parabolic Lipschitz graph.

Local tangents glue to form a graph with Carleson estimate

Whitney decomposition. Cover $V \cap P(\mathbf{0}, 1)$ by parabolic balls $\{P(\mathbf{y}, \mathbf{r_y})\}$ where $\mathbf{y}$ is $\mathcal{C}_+$ projected to V.

Local graph pieces. On each $P(\mathbf{y}, c\mathbf{r_y})$ choose a best k-plane $V_\mathbf{y}$ and write a local graph map $G_\mathbf{y}$ whose graph tracks $\mathcal{C}$ there.

Glue with a partition of unity. With $\{\phi_\mathbf{y}\}$ subordinate to $\{P(\mathbf{y}, \mathbf{r_y})\}$.

$$G := \sum_{\mathbf{y}} \phi_\mathbf{y} \, G_\mathbf{y}.$$

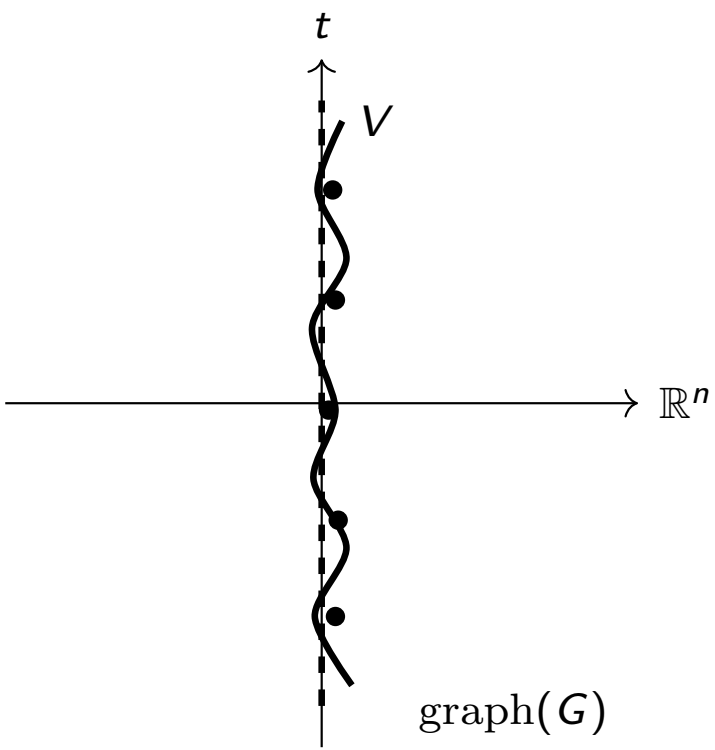

Parabolic refinement. A Carleson estimate for κ yields $\|\partial_t^{1/2} G\|_{\mathrm{BMO}_P} \lesssim$ (small), **so G is regular parabolic Lipschitz**.

For $k \in \{n, n+1\}$, $\mathcal{S}^k_{\epsilon,r}$ on a *strong* neck region is contained in a regular parabolic Lipschitz graph.

Organizing points by multiscale polynomial symmetry

We decompose points according to whether, across many scales, they exhibit k symmetries or an additional $(k+1)$th symmetry.

Let $k \in \{n, n+1\}$ and assume $N_{\mathbf{0}}(\gamma^{-100}) \leq \Lambda$. For any $\varepsilon \in (0,1]$ and $\eta \leq \eta(\Lambda)$, there exists a decomposition

$$P(\mathbf{0},1) \subseteq \bigcup_a \mathcal{N}_a \cup \bigcup_b P(\mathbf{x}_b, r_b) \cup \left(\widetilde{\mathcal{C}} \cup \bigcup_a \mathcal{C}_{a,0} \right).$$

- Each $\mathcal{N}_a$ is a strong neck region.
- For each ball $P(\mathbf{x}_b, r_b)$, the function u is almost $(k+1)$-symmetric at some point $y_b \in P(\mathbf{x}_b, r_b)$.
- If $k = n+1$, then
$$\mathcal{Z}(u) \in \mathcal{C}_{\mathrm{sing}}(n-1).$$
- If $k = n$, then
$$\mathcal{S}(u) \in \mathcal{C}_{\mathrm{sing}}(n-1).$$

Organizing points by multiscale polynomial symmetry

We decompose points according to whether, across many scales, they exhibit k symmetries or an additional $(k+1)$th symmetry.

Let $k \in \{n, n+1\}$ and assume $N_{\mathbf{0}}(\gamma^{-100}) \leq \Lambda$. For any $\varepsilon \in (0,1]$ and $\eta \leq \eta(\Lambda)$, there exists a decomposition

$$P(\mathbf{0},1) \subseteq \bigcup_a \mathcal{N}_a \cup \bigcup_b P(\mathbf{x}_b, r_b) \cup \left(\widetilde{\mathcal{C}} \cup \bigcup_a \mathcal{C}_{a,0} \right).$$

- Each $\mathcal{N}_a$ is a strong neck region.
- For each ball $P(\mathbf{x}_b, r_b)$, the function u is almost $(k+1)$-symmetric at some point $\mathbf{y}_b \in P(\mathbf{x}_b, r_b)$.
- If $k = n+1$, then

$$Z(u) \subset \widetilde{\mathcal{C}} \cup \bigcup_a \mathcal{C}_{a,0},$$

while if $k = n$, then

$$S(u) \subset \widetilde{\mathcal{C}} \cup \bigcup_a \mathcal{C}_{a,0}.$$

Organizing points by multiscale polynomial symmetry

We decompose points according to whether, across many scales, they exhibit k symmetries or an additional $(k+1)$th symmetry.

Let $k \in \{n, n+1\}$ and assume $N_{\mathbf{0}}(\gamma^{-100}) \leq \Lambda$. For any $\varepsilon \in (0,1]$ and $\eta \leq \eta(\Lambda)$, there exists a decomposition

$$P(\mathbf{0},1) \subseteq \bigcup_a \mathcal{N}_a \cup \bigcup_b P(\mathbf{x}_b, r_b) \cup \left(\widetilde{\mathcal{C}} \cup \bigcup_a \mathcal{C}_{a,0} \right).$$

- Each $\mathcal{N}_a$ is a strong neck region.
- For each ball $P(\mathbf{x}_b, r_b)$, the function u is almost $(k+1)$-symmetric at some point $\mathbf{y}_b \in P(\mathbf{x}_b, r_b)$.
- If $k = n+1$, then

$$Z(u) \subset \widetilde{\mathcal{C}} \cup \bigcup_a \mathcal{C}_{a,0},$$

while if $k = n$, then

$$S(u) \subset \widetilde{\mathcal{C}} \cup \bigcup_a \mathcal{C}_{a,0}.$$

Organizing points by multiscale polynomial symmetry

We decompose points according to whether, across many scales, they exhibit k symmetries or an additional $(k+1)$th symmetry.

Let $k \in \{n, n+1\}$ and assume $N_{\mathbf{0}}(\gamma^{-100}) \leq \Lambda$. For any $\varepsilon \in (0,1]$ and $\eta \leq \eta(\Lambda)$, there exists a decomposition

$$P(\mathbf{0},1) \subseteq \bigcup_a \mathcal{N}_a \cup \bigcup_b P(\mathbf{x}_b, r_b) \cup \left(\widetilde{\mathcal{C}} \cup \bigcup_a \mathcal{C}_{a,0} \right).$$

- Each $\mathcal{N}_a$ is a strong neck region.
- For each ball $P(\mathbf{x}_b, r_b)$, the function u is almost $(k+1)$-symmetric at some point $\mathbf{y}_b \in P(\mathbf{x}_b, r_b)$.
- If $k = n+1$, then

$$Z(u) \subset \widetilde{\mathcal{C}} \cup \bigcup_a \mathcal{C}_{a,0},$$

while if $k = n$, then

$$S(u) \subset \widetilde{\mathcal{C}} \cup \bigcup_a \mathcal{C}_{a,0}.$$

Finite-resolution neck decomposition

Fix a resolution $r_* \in (0, 1]$. Given $\epsilon, \eta, r_*, \Lambda$, there is a cover of the unit parabolic ball:

$$P(\mathbf{0}, 1) \subset \bigcup_a \mathcal{N}_a \cup \bigcup_b P(\mathbf{x}_b, r_b) \cup \bigcup_f P(\mathbf{x}_f, r_f).$$

- $\mathcal{N}_a = P(\mathbf{x}_a, 2r_a) \setminus P(\mathcal{C}_a, r_\bullet)$ is a neck region, with $r_\bullet \geq r_*$.
- u is almost $k+1$-symmetric at some $\mathbf{y}_b \in P(\mathbf{x}_b, r_b)$.
- $r_a, r_b \geq r_*$ and $r_f \in [r_*, C(\Lambda, \varepsilon, \eta)\, r_*]$ so all residual pieces are commensurable to r_*.
- $\sum_a r_a^k + \sum_b r_b^k + \sum_f r_f^k \leq C(\Lambda)\,(\varepsilon\eta)^{-C(\Lambda)}$.

Why "finite resolution"? Unlike earlier neck decompositions, the residual cannot be thrown away by approximating u with a nicer solution: we must keep a leftover region *at scale* r_* to obtain Minkowski bounds at resolution r_*.

Finite-resolution neck decomposition

Fix a resolution $r_* \in (0, 1]$. Given $\epsilon, \eta, r_*, \Lambda$, there is a cover of the unit parabolic ball:

$$P(\mathbf{0}, 1) \subset \bigcup_a \mathcal{N}_a \cup \bigcup_b P(\mathbf{x}_b, r_b) \cup \bigcup_f P(\mathbf{x}_f, r_f).$$

- $\mathcal{N}_a = P(\mathbf{x}_a, 2r_a) \setminus P(\mathcal{C}_a, r_\bullet)$ is a neck region, with $r_\bullet \geq r_*$.
- u is almost $k+1$-symmetric at some $\mathbf{y}_b \in P(\mathbf{x}_b, r_b)$.
- $r_a, r_b \geq r_*$ and $r_f \in [r_*, C(\Lambda, \varepsilon, \eta)\, r_*]$ so all residual pieces are commensurable to r_*.
- $\sum_a r_a^k + \sum_b r_b^k + \sum_f r_f^k \leq C(\Lambda)\,(\varepsilon\eta)^{-C(\Lambda)}$.

Why "finite resolution"? Unlike earlier neck decompositions, the residual cannot be thrown away by approximating u with a nicer solution: we must keep a leftover region *at scale* r_* to obtain Minkowski bounds at resolution r_*.

Finite-resolution neck decomposition

Fix a resolution $r_* \in (0, 1]$. Given $\epsilon, \eta, r_*, \Lambda$, there is a cover of the unit parabolic ball:

$$P(\mathbf{0}, 1) \subset \bigcup_a \mathcal{N}_a \cup \bigcup_b P(\mathbf{x}_b, r_b) \cup \bigcup_f P(\mathbf{x}_f, r_f).$$

- $\mathcal{N}_a = P(\mathbf{x}_a, 2r_a) \setminus P(\mathcal{C}_a, r_\bullet)$ is a neck region, with $r_\bullet \geq r_*$.
- u is almost $k+1$-symmetric at some $\mathbf{y}_b \in P(\mathbf{x}_b, r_b)$.
- $r_a, r_b \geq r_*$ and $r_f \in [r_*,\ C(\Lambda, \varepsilon, \eta)\, r_*]$ so all residual pieces are commensurable to r_*.
- $\sum_a r_a^k + \sum_b r_b^k + \sum_f r_f^k \leq C(\Lambda)\,(\varepsilon\eta)^{-C(\Lambda)}$.

Why "finite resolution"? Unlike earlier neck decompositions, the residual cannot be thrown away by approximating u with a nicer solution: we must keep a leftover region *at scale* r_* to obtain Minkowski bounds at resolution r_*.

Finite-resolution neck decomposition

Fix a resolution $r_* \in (0, 1]$. Given $\epsilon, \eta, r_*, \Lambda$, there is a cover of the unit parabolic ball:

$$P(\mathbf{0}, 1) \subset \bigcup_a \mathcal{N}_a \cup \bigcup_b P(\mathbf{x}_b, r_b) \cup \bigcup_f P(\mathbf{x}_f, r_f).$$

- $\mathcal{N}_a = P(\mathbf{x}_a, 2r_a) \setminus P(\mathcal{C}_a, r_\bullet)$ is a neck region, with $r_\bullet \geq r_*$.
- u is almost $k+1$-symmetric at some $\mathbf{y}_b \in P(\mathbf{x}_b, r_b)$.
- $r_a, r_b \geq r_*$ and $r_f \in [r_*, C(\Lambda, \varepsilon, \eta)\, r_*]$ so all residual pieces are commensurable to r_*.
- $\sum_a r_a^k + \sum_b r_b^k + \sum_f r_f^k \leq C(\Lambda)\,(\varepsilon\eta)^{-C(\Lambda)}$.

Why "finite resolution"? Unlike earlier neck decompositions, the residual cannot be thrown away by approximating u with a nicer solution: we must keep a leftover region *at scale* r_* to obtain Minkowski bounds at resolution r_*.

Finite-resolution neck decomposition

Fix a resolution $r_* \in (0, 1]$. Given $\epsilon, \eta, r_*, \Lambda$, there is a cover of the unit parabolic ball:

$$P(\mathbf{0}, 1) \subset \bigcup_a \mathcal{N}_a \cup \bigcup_b P(\mathbf{x}_b, r_b) \cup \bigcup_f P(\mathbf{x}_f, r_f).$$

- $\mathcal{N}_a = P(\mathbf{x}_a, 2r_a) \setminus P(\mathcal{C}_a, r_\bullet)$ is a neck region, with $r_\bullet \geq r_*$.
- u is almost $k+1$-symmetric at some $\mathbf{y}_b \in P(\mathbf{x}_b, r_b)$.
- $r_a, r_b \geq r_*$ and $r_f \in [r_*, C(\Lambda, \varepsilon, \eta)\, r_*]$ so all residual pieces are commensurable to r_*.
- $\sum_a r_a^k + \sum_b r_b^k + \sum_f r_f^k \leq C(\Lambda)\,(\varepsilon\eta)^{-C(\Lambda)}$.

  Why "finite resolution"? Unlike earlier neck decompositions, the residual cannot be thrown away by approximating u with a nicer solution: we must keep a leftover region *at scale* r_* to obtain Minkowski bounds at resolution r_*.

Main result: regular parabolic Lipschitz graphicality

When $k = n+1$ set $\mathscr{C}^k(u) = Z(u)$ and when $k = n$ set $\mathscr{C}^k(u) = S(u)$.
Most of $\mathscr{C}^k(u)$ is organized along **regular parabolic Lipschitz graphs** over vertical affine subspaces of dimension k.

Theorem

Let u be a caloric function with $N(10^5) \leq \Lambda$. For any $k \in \{n, n+1\}$ and $\epsilon > 0$, there exist $\mathbf{x}_i \in P(\mathbf{0}, \frac{1}{4})$, vertical planes $V_i \in \mathrm{Aff}_{\mathcal{P}}(k)$, $r_i \in (0,1]$, and ϵ-regular parabolic Lipschitz functions $F_i : V_i \to V_i^{\perp}$ such that $\sum_i r_i^k \leq C(\epsilon, \Lambda)$, and such that $G_i := \{\mathbf{x} + F_i(\mathbf{x}) : \mathbf{x} \in V_i \cap P(\mathbf{x}_i, 10r_i)\}$ satisfy

$$\mathcal{H}^k_{\mathcal{P}}\left((P(\mathbf{0},1) \cap \mathscr{C}^k(u)) \setminus \bigcup_i G_i \right) = 0.$$

Main result: regular parabolic Lipschitz graphicality

When $k = n+1$ set $\mathscr{C}^k(u) = Z(u)$ and when $k = n$ set $\mathscr{C}^k(u) = S(u)$.
Most of $\mathscr{C}^k(u)$ is organized along **regular parabolic Lipschitz graphs** over vertical affine subspaces of dimension k.

Theorem

Let u be a caloric function with $N(10^5) \leq \Lambda$. For any $k \in \{n, n+1\}$ and $\epsilon > 0$, there exist $\mathbf{x}_i \in P(\mathbf{0}, \frac{1}{4})$, vertical planes $V_i \in \mathrm{Aff}_{\mathcal{P}}(k)$, $r_i \in (0,1]$, and ϵ-regular parabolic Lipschitz functions $F_i \colon V_i \to V_i^{\perp}$ such that $\sum_i r_i^k \leq C(\epsilon, \Lambda)$, and such that $G_i := \{\mathbf{x} + F_i(\mathbf{x}) \colon \mathbf{x} \in V_i \cap P(\mathbf{x}_i, 10r_i)\}$ satisfy

$$\mathcal{H}^k_{\mathcal{P}}\left((P(\mathbf{0},1) \cap \mathscr{C}^k(u)) \setminus \bigcup_i G_i \right) = 0.$$

Main result: Codimension 1 and 2 minkowski estimate

Theorem

Let $k \in \{n, n+1\}$ and let u be a caloric function with $N(10^5) \leq \Lambda$. Then, for any $r \in (0, 1]$,

$$\mathcal{H}^{n+2}_{\mathcal{P}}(P(\mathscr{C}^k_r(u), r) \cap P(\mathbf{0}, 1)) \leq C^{\Lambda^4} r^{n+2-k}.$$

Volume say $\mathscr{C}^k$ is k dimensional. We expect the dependence on Λ is not optimal. It is polynomial on Λ in the elliptic setting.

Corollary

1. *For $\mathcal{H}^{\frac{1}{2}}$-almost every $t \in (-1, 1)$, $\mathscr{C}^k_t(u) := \mathscr{C}^k(u) \cap (B(0^n, 1) \times \{t\})$ satisfies $\mathcal{H}^{k-1}(\mathscr{C}^k_t(u)) = 0$.*
2. *For $\mathcal{H}^1$-almost every $t \in (-1, 1)$, $\mathscr{C}^k_t(u)$ is $(k-2)$-rectifiable, and $\mathcal{H}^{k-2}(\mathscr{C}^k_t(u)) \leq C^{\Lambda^4}$.*

Estimate for S_t can't be improved for all time slices since $S_0(u) = Z_0(u) = \{(0, 0)\}$ when $u = x^2 + 2t$.

Main result: Codimension 1 and 2 minkowski estimate

Theorem

Let $k \in \{n, n+1\}$ and let u be a caloric function with $N(10^5) \leq \Lambda$. Then, for any $r \in (0, 1]$,

$$\mathcal{H}^{n+2}_{\mathcal{P}}(P(\mathscr{C}^k_r(u), r) \cap P(\mathbf{0}, 1)) \leq C^{\Lambda^4} r^{n+2-k}.$$

Volume say $\mathscr{C}^k$ is k dimensional. We expect the dependence on Λ is not optimal. It is polynomial on Λ in the elliptic setting.

Corollary

1. *For $\mathcal{H}^{\frac{1}{2}}$-almost every $t \in (-1, 1)$, $\mathscr{C}^k_t(u) := \mathscr{C}^k(u) \cap (B(0^n, 1) \times \{t\})$ satisfies $\mathcal{H}^{k-1}(\mathscr{C}^k_t(u)) = 0$.*
2. *For $\mathcal{H}^1$-almost every $t \in (-1, 1)$, $\mathscr{C}^k_t(u)$ is $(k-2)$-rectifiable, and $\mathcal{H}^{k-2}(\mathscr{C}^k_t(u)) \leq C^{\Lambda^4}$.*

Estimate for S_t can't be improved for all time slices since $S_0(u) = Z_0(u) = \{(0, 0)\}$ when $u = x^2 + 2t$.

Main result: Codimension 1 and 2 minkowski estimate

Theorem

Let $k \in \{n, n+1\}$ and let u be a caloric function with $N(10^5) \leq \Lambda$. Then, for any $r \in (0, 1]$,

$$\mathcal{H}^{n+2}_{\mathcal{P}}(P(\mathscr{C}^k_r(u), r) \cap P(\mathbf{0}, 1)) \leq C^{\Lambda^4} r^{n+2-k}.$$

Volume say $\mathscr{C}^k$ is k dimensional. We expect the dependence on Λ is not optimal. It is polynomial on Λ in the elliptic setting.

Corollary

1. *For $\mathcal{H}^{\frac{1}{2}}$-almost every $t \in (-1, 1)$, $\mathscr{C}^k_t(u) := \mathscr{C}^k(u) \cap (B(0^n, 1) \times \{t\})$ satisfies $\mathcal{H}^{k-1}(\mathscr{C}^k_t(u)) = 0$.*
2. *For $\mathcal{H}^1$-almost every $t \in (-1, 1)$, $\mathscr{C}^k_t(u)$ is $(k-2)$-rectifiable, and $\mathcal{H}^{k-2}(\mathscr{C}^k_t(u)) \leq C^{\Lambda^4}$.*

Estimate for S_t can't be improved for all time slices since $S_0(u) = Z_0(u) = \{(0, 0)\}$ when $u = x^2 + 2t$.

Main result: Codimension 1 and 2 minkowski estimate

Theorem

Let $k \in \{n, n+1\}$ and let u be a caloric function with $N(10^5) \leq \Lambda$. Then, for any $r \in (0, 1]$,

$$\mathcal{H}^{n+2}_{\mathcal{P}}(P(\mathscr{C}^k_r(u), r) \cap P(\mathbf{0}, 1)) \leq C^{\Lambda^4} r^{n+2-k}.$$

Volume say $\mathscr{C}^k$ is k dimensional. We expect the dependence on Λ is not optimal. It is polynomial on Λ in the elliptic setting.

Corollary

1. *For $\mathcal{H}^{\frac{1}{2}}$-almost every $t \in (-1, 1)$, $\mathscr{C}^k_t(u) := \mathscr{C}^k(u) \cap (B(0^n, 1) \times \{t\})$ satisfies $\mathcal{H}^{k-1}(\mathscr{C}^k_t(u)) = 0$.*
2. *For $\mathcal{H}^1$-almost every $t \in (-1, 1)$, $\mathscr{C}^k_t(u)$ is $(k-2)$-rectifiable, and $\mathcal{H}^{k-2}(\mathscr{C}^k_t(u)) \leq C^{\Lambda^4}$.*

Estimate for S_t can't be improved for all time slices since $S_0(u) = Z_0(u) = \{(0, 0)\}$ when $u = x^2 + 2t$.

Recap of the argument in the caloric setting

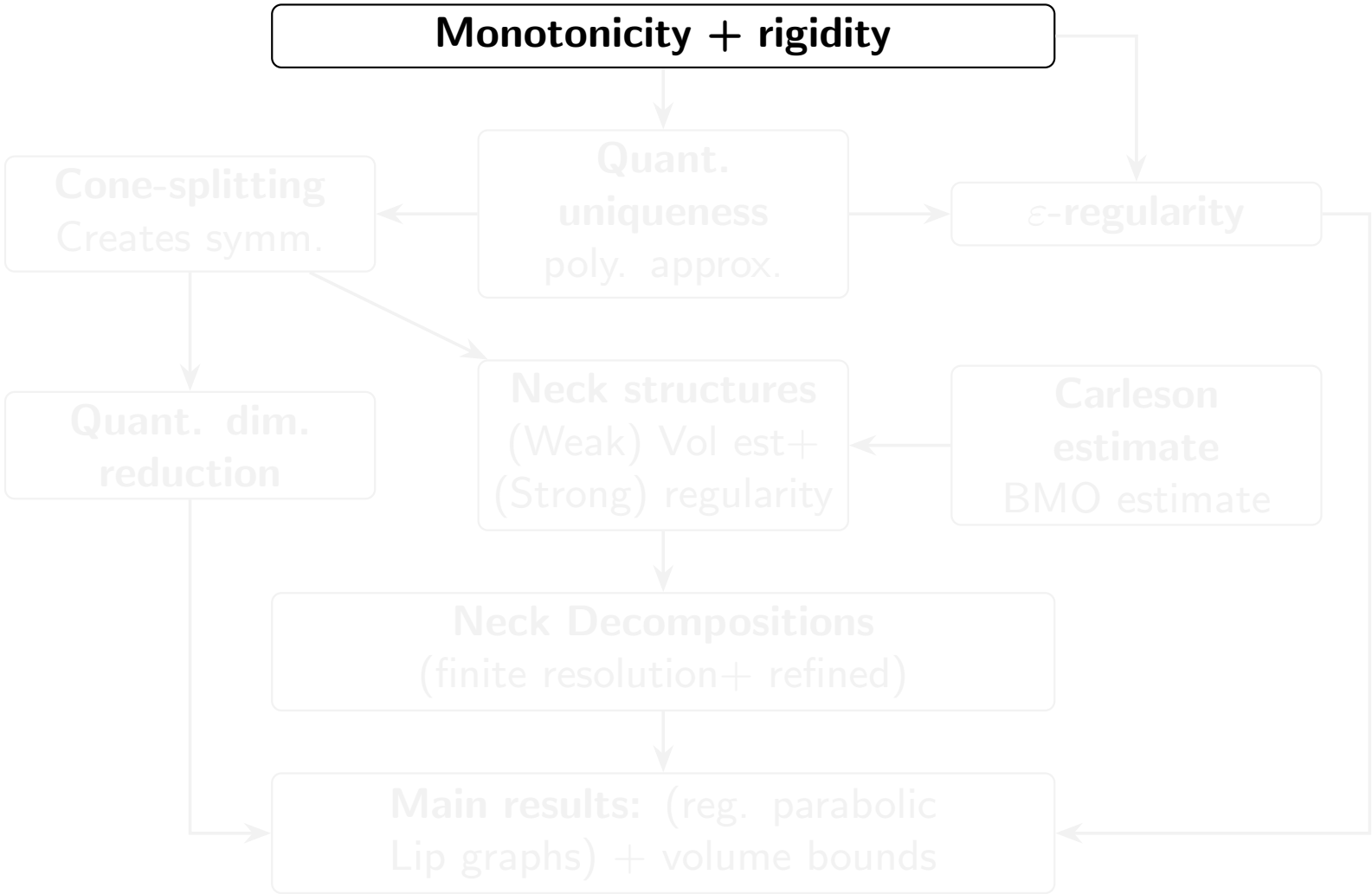

They say it's all about location, location location! I say it's about location, scale and resolution!

Recap of the argument in the caloric setting

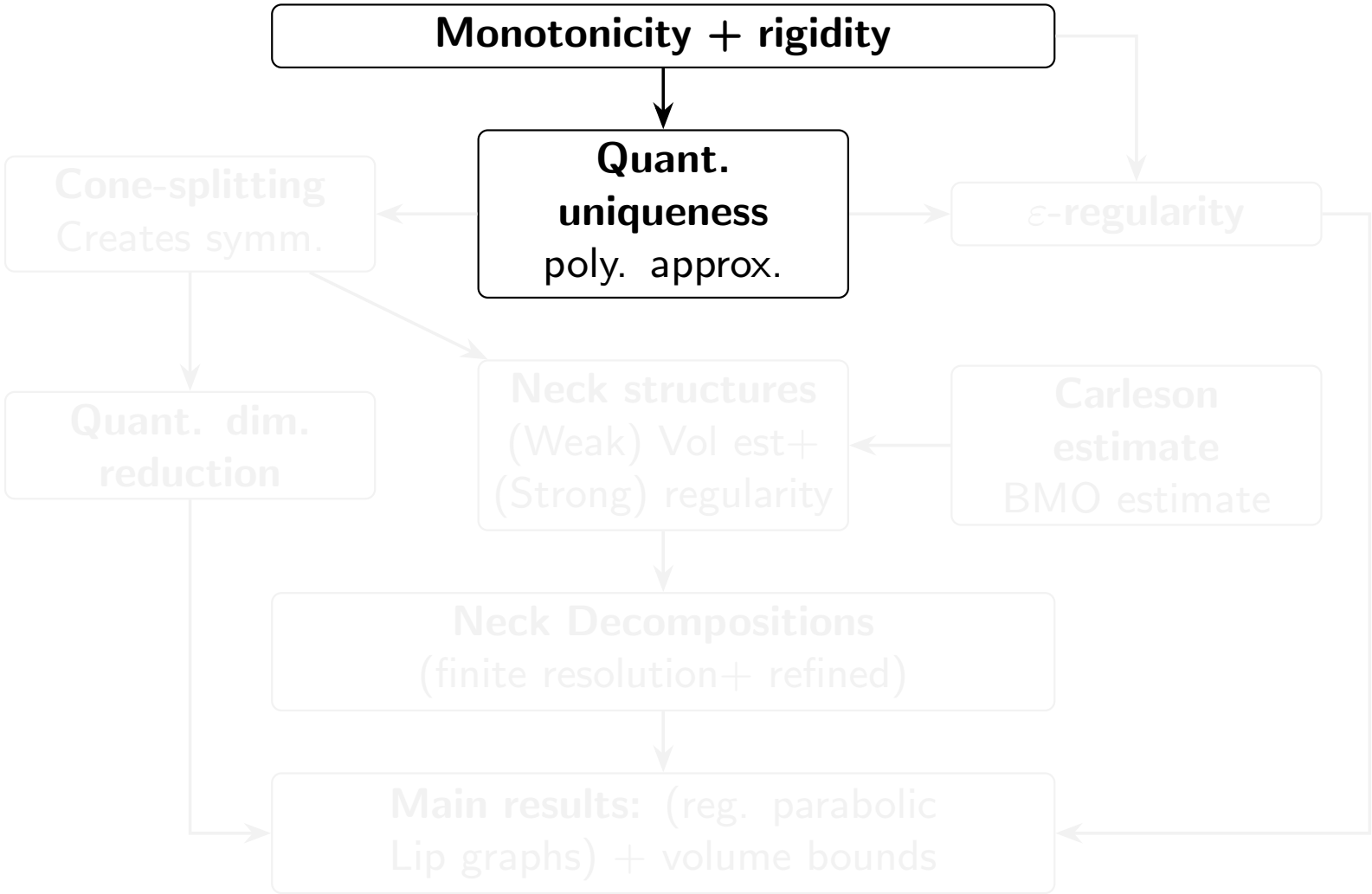

They say it's all about location, location location! I say it's about location, scale and resolution!

Recap of the argument in the caloric setting

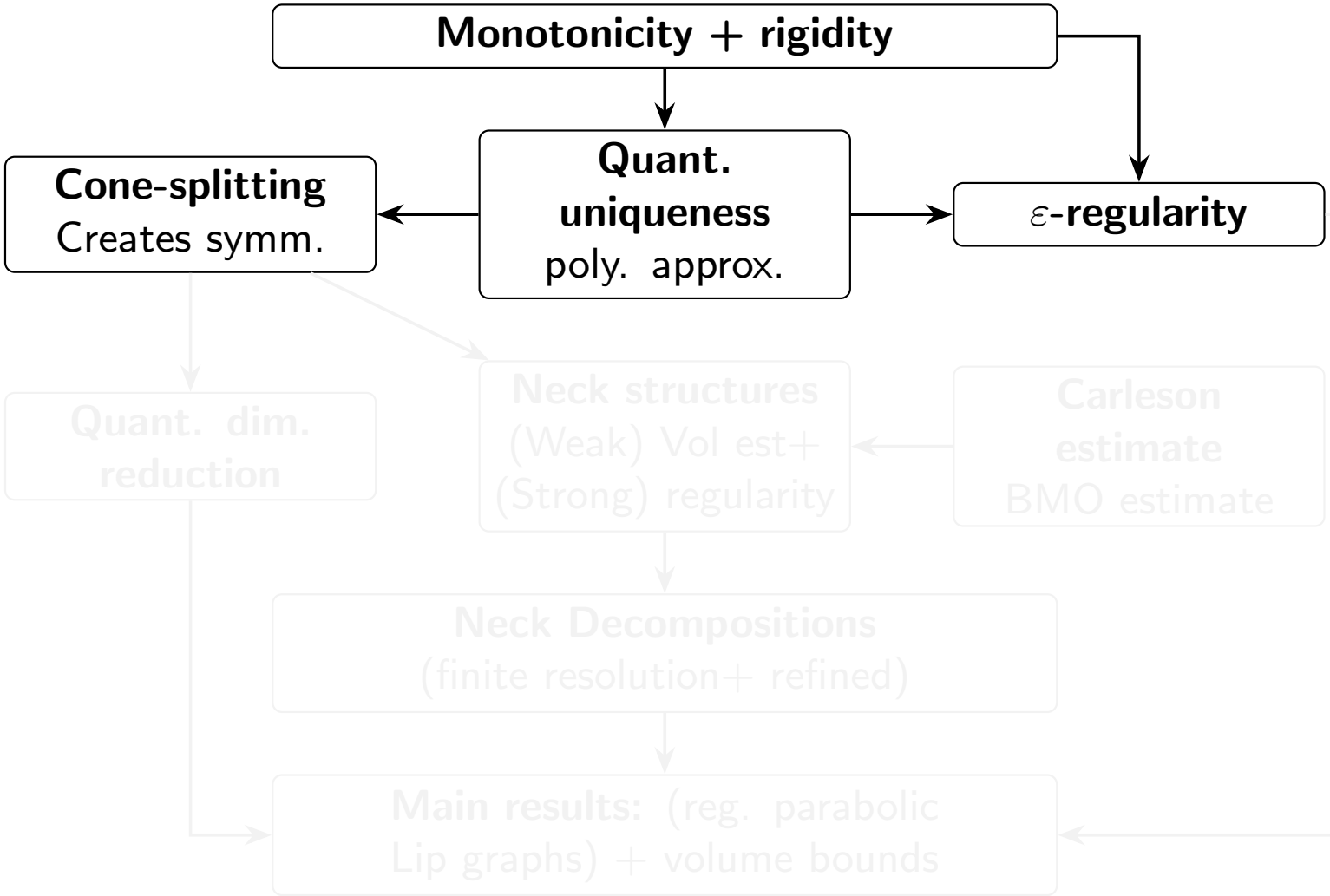

They say it's all about location, location location! I say it's about location, scale and resolution!

Recap of the argument in the caloric setting

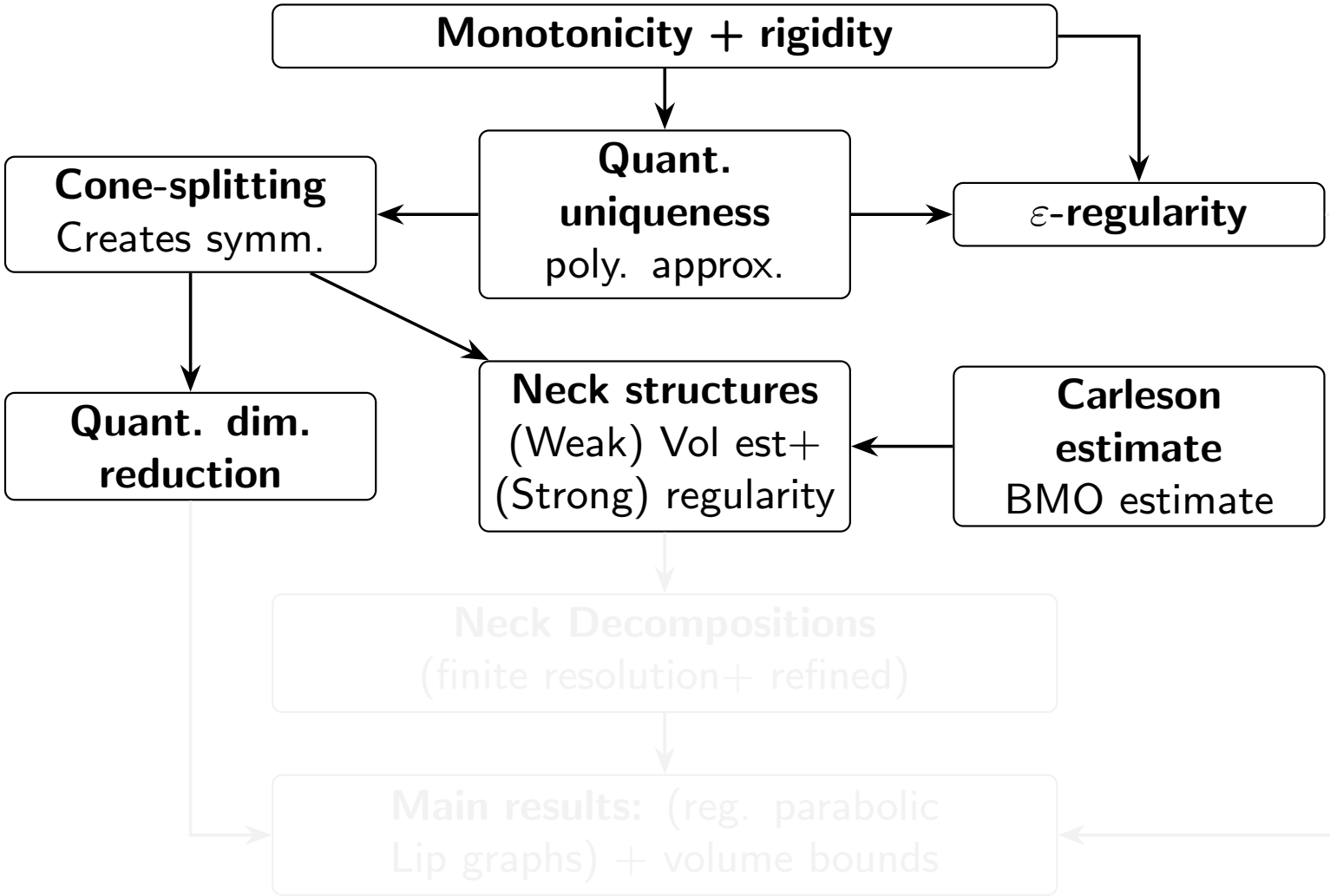

They say it's all about location, location location! I say it's about location, scale and resolution!

Recap of the argument in the caloric setting

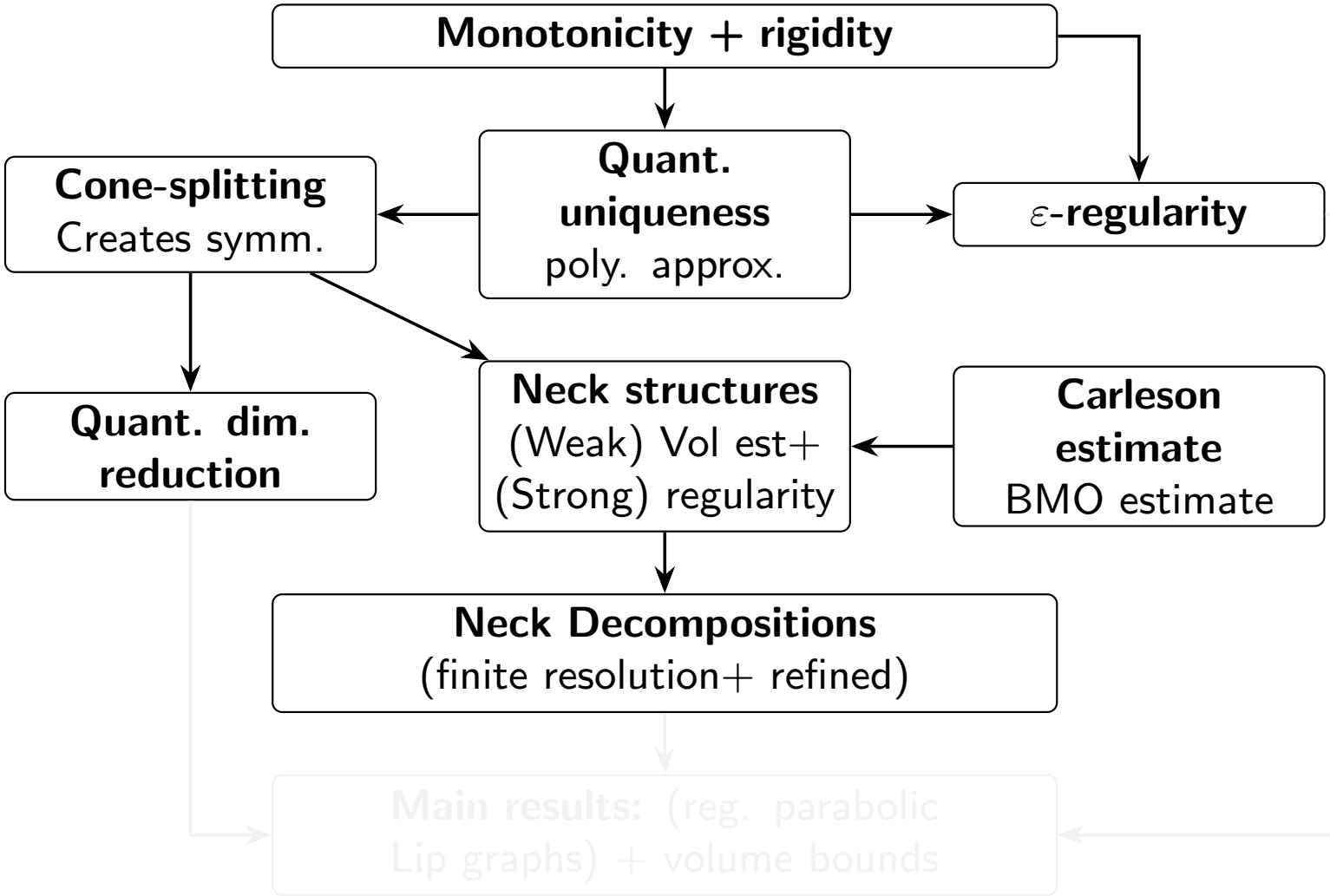

They say it's all about location, location location! I say it's about location, scale and resolution!

Recap of the argument in the caloric setting

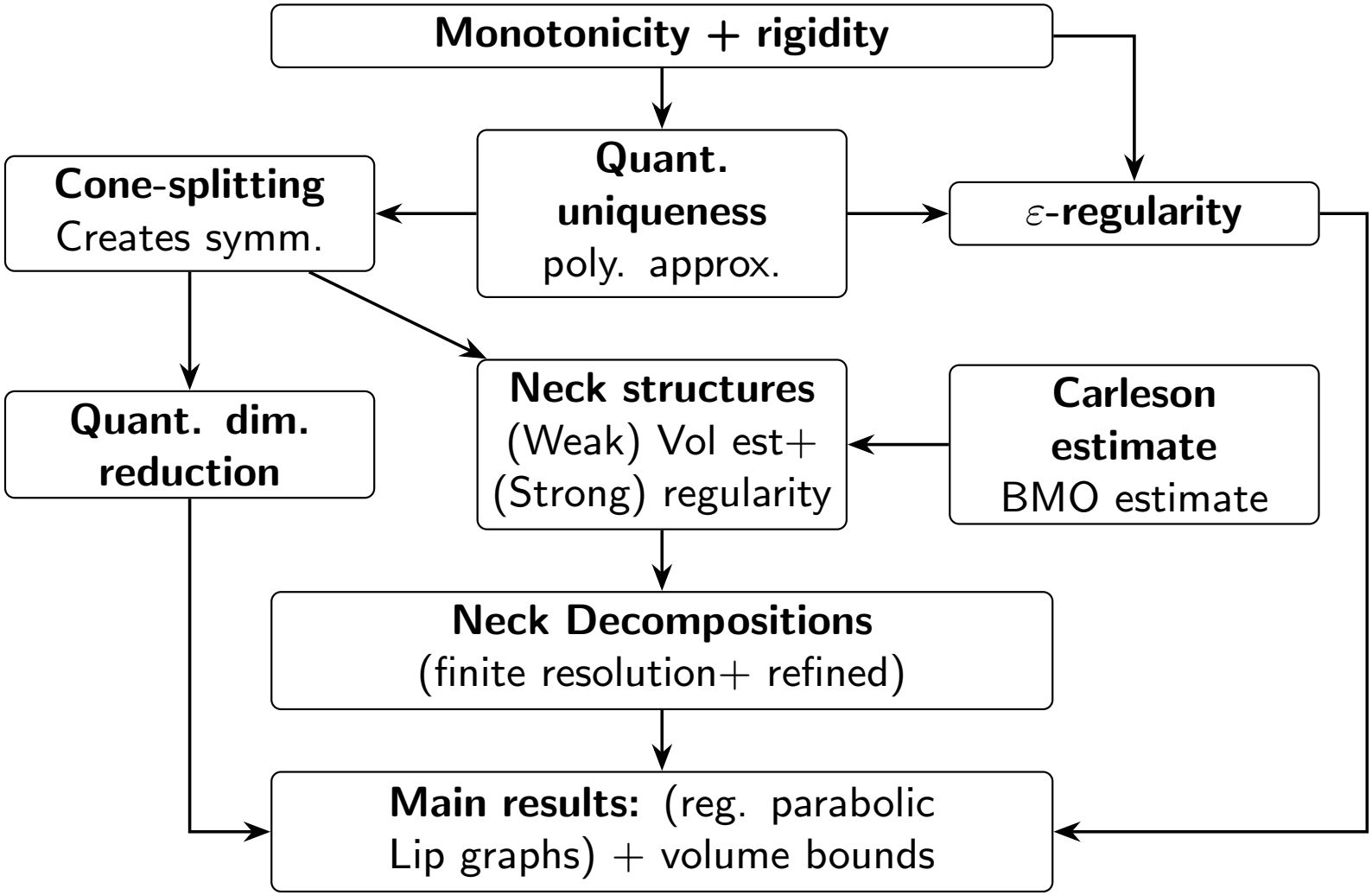

They say it's all about location, location location! I say it's about location, scale and resolution!

Recap of the argument in the caloric setting

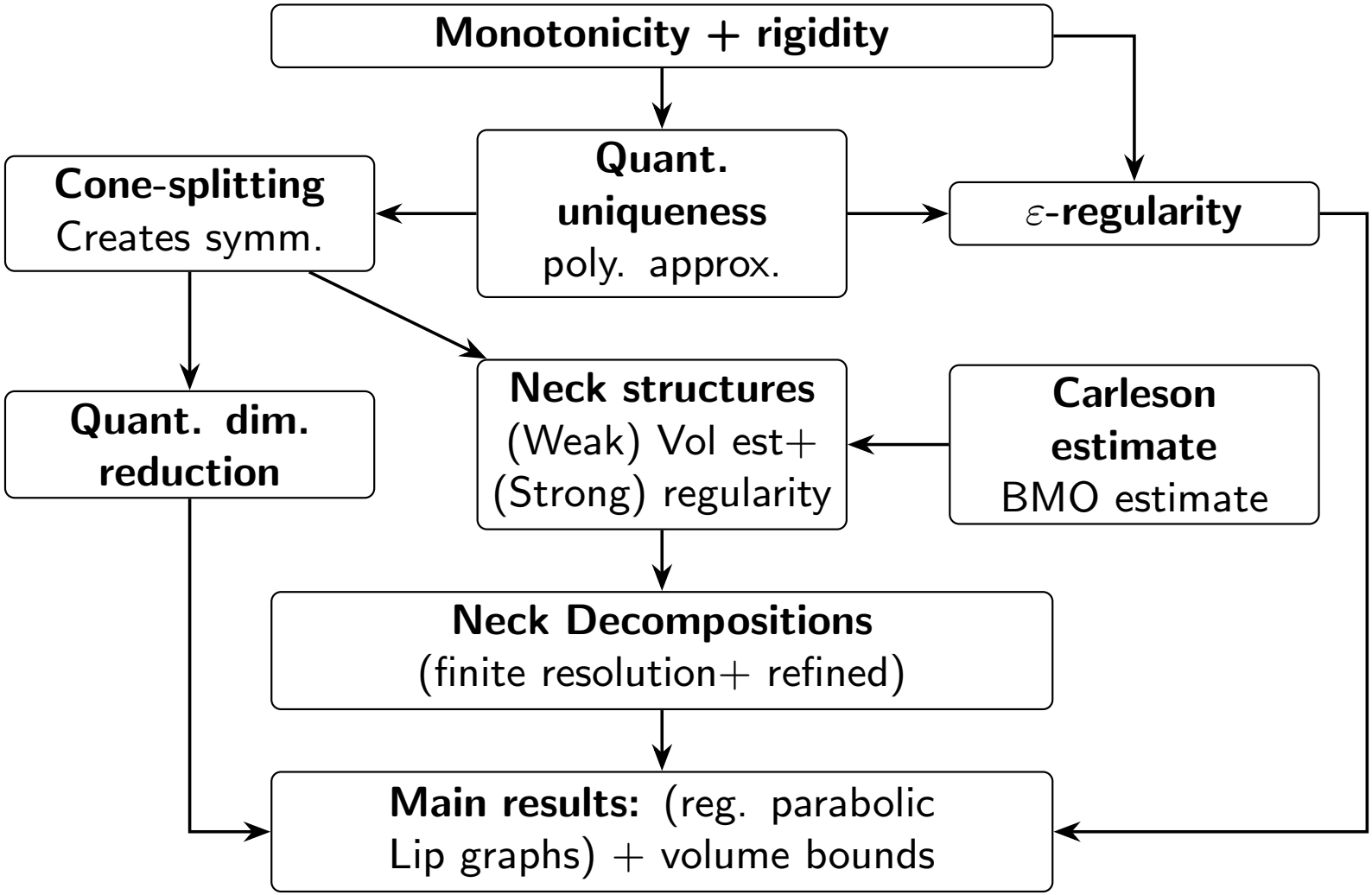

They say it's all about location, location location! I say it's about location, scale and resolution!

General setup: errors summable across scales

Recall, general setting of parabolic inequality with Lipschitz coefficients (on a parabolic ball)+ doubling coefficients.

For global functions, we have

$$N'_{\mathbf{x}_0}(\tau) = \frac{4\tau}{H_{\mathbf{x}_0}(\tau)} \int_{\mathbb{R}^n} \left(\left(\Delta_{f_{\mathbf{x}_0}} u + \frac{N_{\mathbf{x}_0}(\tau)}{2\tau} u \right)^2 + \left(\Delta_{f_{\mathbf{x}_0}} u + \frac{N_{\mathbf{x}_0}(\tau)}{2\tau} u \right) \Box u \right) d\nu_{\mathbf{x}_0;t}.$$

- The second term is a scale/M-dependent error term to that arises a perturbation of caloric function, u is almost $\mathfrak{w}$-monotone. Another source of error comes from using a cutoff because u is not global.
- Quantitative uniqueness is not straightforward. Need to do stability analysis of dynamical rescaling.
- For rest of the tools, the geometric steps survives, but we must always track PDE errors. Caloric approximation saves us.
- Use doubling condition to get polynomial growth of solutions to the exponential tail of Gaussian to control error terms that are summable across scales for Carleman estimate.

General setup: errors summable across scales

Recall, general setting of parabolic inequality with Lipschitz coefficients (on a parabolic ball)+ doubling coefficients.
For global functions, we have

$$N'_{\mathbf{x}_0}(\tau) = \frac{4\tau}{H_{\mathbf{x}_0}(\tau)} \int_{\mathbb{R}^n} \left(\left(\Delta_{f_{\mathbf{x}_0}} u + \frac{N_{\mathbf{x}_0}(\tau)}{2\tau} u \right)^2 + \left(\Delta_{f_{\mathbf{x}_0}} u + \frac{N_{\mathbf{x}_0}(\tau)}{2\tau} u \right) \Box u \right) d\nu_{\mathbf{x}_0;t}.$$

General setup: errors summable across scales

Recall, general setting of parabolic inequality with Lipschitz coefficients (on a parabolic ball)+ doubling coefficients.
For global functions, we have

$$N'_{\mathbf{x}_0}(\tau) = \frac{4\tau}{H_{\mathbf{x}_0}(\tau)} \int_{\mathbb{R}^n} \left(\left(\Delta_{f_{\mathbf{x}_0}} u + \frac{N_{\mathbf{x}_0}(\tau)}{2\tau} u \right)^2 + \left(\Delta_{f_{\mathbf{x}_0}} u + \frac{N_{\mathbf{x}_0}(\tau)}{2\tau} u \right) \Box u \right) d\nu_{\mathbf{x}_0;t}.$$

- The **second term is a scale/M-dependent error** term so that if u is a perturbation of caloric function, N is **almost monotone.** Another source of error comes from using a **cutoff** because u is not global.
- Quantitative uniqueness is not straightforward. Need to do **stability analysis** of dynamical rescaling.
- For rest of the tools, the **geometric step survives,** but we must absorb PDE errors. Caloric approximation saves us.

  Fixes Use doubling condition to get **polynomial growth of solutions** u and the **exponential tail of Gaussian** to control **error terms** so that they are **summable across scales for Carleson estimate.** And it works!!!

General setup: errors summable across scales

Recall, general setting of parabolic inequality with Lipschitz coefficients (on a parabolic ball)+ doubling coefficients.
For global functions, we have

$$N'_{\mathbf{x}_0}(\tau) = \frac{4\tau}{H_{\mathbf{x}_0}(\tau)} \int_{\mathbb{R}^n} \left(\left(\Delta_{f_{\mathbf{x}_0}} u + \frac{N_{\mathbf{x}_0}(\tau)}{2\tau} u \right)^2 + \left(\Delta_{f_{\mathbf{x}_0}} u + \frac{N_{\mathbf{x}_0}(\tau)}{2\tau} u \right) \Box u \right) d\nu_{\mathbf{x}_0;t}.$$

- The **second term is a scale/M-dependent error** term so that if u is a perturbation of caloric function, N is **almost monotone.** Another source of error comes from using a **cutoff** because u is not global.
- Quantitative uniqueness is not straightforward. Need to do **stability analysis** of dynamical rescaling.
- For rest of the tools, the **geometric step survives,** but we must absorb PDE errors. Caloric approximation saves us.

  Fixes Use doubling condition to get **polynomial growth of solutions** u and the **exponential tail of Gaussian** to control **error terms** so that they are **summable across scales for Carleson estimate.** And it works!!!

General setup: errors summable across scales

Recall, general setting of parabolic inequality with Lipschitz coefficients (on a parabolic ball)+ doubling coefficients.
For global functions, we have

$$N'_{\mathbf{x}_0}(\tau) = \frac{4\tau}{H_{\mathbf{x}_0}(\tau)} \int_{\mathbb{R}^n} \left(\left(\Delta_{f_{\mathbf{x}_0}} u + \frac{N_{\mathbf{x}_0}(\tau)}{2\tau} u \right)^2 + \left(\Delta_{f_{\mathbf{x}_0}} u + \frac{N_{\mathbf{x}_0}(\tau)}{2\tau} u \right) \Box u \right) d\nu_{\mathbf{x}_0;t}.$$

- The **second term is a scale/M-dependent error** term so that if u is a perturbation of caloric function, N is **almost monotone.** Another source of error comes from using a **cutoff** because u is not global.
- Quantitative uniqueness is not straightforward. Need to do **stability analysis** of dynamical rescaling.
- For rest of the tools, the **geometric step survives,** but we must absorb PDE errors. Caloric approximation saves us.

Fixes Use doubling condition to get **polynomial growth of solutions** u and the **exponential tail of Gaussian** to control **error terms** so that they are **summable across scales for Carleson estimate.** And it works!!!

General setup: errors summable across scales

Recall, general setting of parabolic inequality with Lipschitz coefficients (on a parabolic ball)+ doubling coefficients.
For global functions, we have

$$N'_{\mathbf{x}_0}(\tau) = \frac{4\tau}{H_{\mathbf{x}_0}(\tau)} \int_{\mathbb{R}^n} \left(\left(\Delta_{f_{\mathbf{x}_0}} u + \frac{N_{\mathbf{x}_0}(\tau)}{2\tau} u \right)^2 + \left(\Delta_{f_{\mathbf{x}_0}} u + \frac{N_{\mathbf{x}_0}(\tau)}{2\tau} u \right) \Box u \right) d\nu_{\mathbf{x}_0;t}.$$

- The **second term is a scale/M-dependent error** term so that if u is a perturbation of caloric function, N is **almost monotone.** Another source of error comes from using a **cutoff** because u is not global.
- Quantitative uniqueness is not straightforward. Need to do **stability analysis** of dynamical rescaling.
- For rest of the tools, the **geometric step survives,** but we must absorb PDE errors. Caloric approximation saves us.

  Fixes Use doubling condition to get **polynomial growth of solutions** u and the **exponential tail of Gaussian** to control **error terms** so that they are **summable across scales for Carleson estimate.** And it works!!!

Thank you!